Tree growth stresses, in situ measurement and properties of normal and reaction woods

Bernard Thibaut, Joseph Gril

Title:

Tree growth stresses, in situ measurement and properties of normal and reaction woods.

Running title: Tree growth stresses

Bernard Thibaut [(1), (*)]

Joseph Gril [(2), (3)]

[(1)] LMGC, Univ Montpellier, CNRS, Montpellier, France

bernard.thibaut@umontpellier.fr

[(*)] Corresponding author

[(2)] Université Clermont Auvergne, CNRS, Sigma Clermont, Institut Pascal, Clermont-Ferrand, France

[(3)] Université Clermont Auvergne, INRAE, PIAF, Clermont Ferrand, France

Highlight

Experimental study of growth stains on trees restoring their verticality after some accidental inclination combined to measuring of wood properties at the same position allows to discuss the functions of forces created by living wood within trees in pre-stressing the woody skeleton on one side, allowing verticality restoration on the other side.

Abstract

Living wood in the tree performs a kind of muscle action generating forces at the sapwood periphery and thus residual strains in the dead sapwood fibres. Dissymmetric force generation around tree trunk is a kind of motor system useful for movement, posture control and tree reshaping after accidents.

Rather young trees are able to restore the verticality of their trunk after accidental rotation of the soil-root system due to wind or some landslide, leading to typical basically curved stems shape. The very high dissymmetry of forces for the motor action is associated with the occurrence of reaction wood on one side of the inclined stem during many successive years.

A selection of 17 such trees coming from 15 different species (13 different families), tropical or temperate, hardwoods or softwoods, were selected and peripheral residual strains were measured in situ before felling, on 8 position for each stem. Associated wooden rods were sawn and measured for their mechanical and physical properties at green and dry state, allowing the estimation of tree growth stresses i.e. forces created by the living wood.

Thanks to the wide range of wood types, species and basic densities, simple and highly significant formulas are found for the relationship between green and dry wood properties such as density, longitudinal modulus of elasticity, specific modulus and two shearing modulus of elasticity. It was also possible to build easy to use conversion coefficients between growth stress indicator (*GSI*), measured in situ by the single hole method, and growth strain and growth stress with the knowledge of basic density and green longitudinal elastic modulus.

Growth strains, specific modulus and longitudinal shrinkage are indicators of the fibre wall properties independent from basic density. Combined to density, they offer a good set of variables in order to study growth strategy (strains and stresses) and important wood properties. Compression wood, normal wood and tension wood describe a continuum for growth strains but do not appear as a continuum for their relationships with the tree indicators. There should be other basic differences separating these wood types, in the chemical composition of the matrix and the ultrastructure of cellulose microfibrils.

Apart from compression wood, density, specific modulus and longitudinal shrinkage are largely inefficient for the prediction of growth stresses and a large experimental study is needed, at first on normal wood only, to investigate chemical determinants of growth stains.

Keywords

Force genesis; growth strains; modulus of elasticity; wood shrinkage; tree biomechanics; wood

Abbreviations and notations

MOE, *MOE*	modulus of elasticity in L direction
E_g	green MOE
E_d	air-dry MOE
E, E_L	Longitudinal modulus
G, G_{TL}, G_{RL}	Shear modulus
ρ	density
BD	basic density
DD	dry density
k	factor for shear contribution (5/6 for rectangular cross section)
SM, *SM*	specific modulus
SMb	basic SM
E_L/ρ	SM in L direction
E_L/G_{TL}, E_L/G_{RL}	anisotropy factor
GSI	growth stress indicator
α_m	maturation strain
σ_m	maturation stress
ϕ	conversion factor αm/GSI
ψ	conversion factor σm/GSI)
L, R, T	longitudinal, radial, tangential directions
L_k, R_k, T_k	dimension in L, R, T direction for condition k
M	mass

DP_x	distance to pith
RH	relative humidity
MC, *MC*	wood moisture content
VS, LS	volumetric, linear shrinkage
FSP	fibre saturation point

Introduction

Tree biomechanics deal with the analysis of mechanical problems encountered by living trees, including multiphysical couplings between the deformations and movements due to external forces and the biology of cell formation and growth. A typical case is the classical experiment of inclining a young tree at the beginning of cambial activity in Spring (Thibaut et al 2001, Thibaut 2019). In agreement with the physics of viscoelastic materials, the immediate response is a downward elastic flexure followed by a slow downward creep flexure during the first 24 hours. But 5 days later the terminal shoot straightens vertically and 3 months later, apart from a significant growth in length at the apical side, the existing stem shows a change of curvature (restoration of verticality) opposite to the physical model prediction. The biological process of wood growth, both in length (primary growth) and in diameter (secondary growth) should be added to the physical model through appropriate biological state variables complementing the physical state variables. Based on the functions of living wood during the three successive phases of cell division, cell wall expansion and cell wall thickening, three sets of biological variables can be set, in relation to geometrical changes, mass changes and force generation.

Geometrical and mass changes are rather well documented in the literature on tree growth (Trouvé et al 2015, Fourcaud et al 2008, Deleuze & Houillier 1997, Chave et al 2005). Their related variables depend on time, genetic growth patterns (architectural model and wood anatomy) and adaption to environment (climate, tree spacing …). Forces are needed to enhance bending strength through pre-stressing (Alméras et al 2018, Gril et al 2017, Thibaut et al 2001) and to create motor systems (Alméras et al 2005b, Alméras & Clair 2016, Coutand et al 2007) allowing posture control (vertical or inclined growth) or tree shape restoration after accidents (apex breaking, rotation of root system …). They are generated during fibre (or tracheid) wall thickening (Mellerowicz et al 2001, Plomion et al 2001, Gorshkova et al 2012) and their level is adapted to the mechanical needs of the tree: high level for slender trees (Loup et al 2013), with a clear asymmetry between two opposite faces of the wooden axis when a motor action is needed (Alméras et al 2005b, Moulia et al 2006, Fournier et al 2014). In the most asymmetrical situation, one side is made of the so-called reaction wood (Gardiner et al 2014), that differs from normal wood in terms of cell wall ultrastructure and chemical composition (Côté & Timell 1969, Dadswell & Wardrop 1955, Timell 1986, Yeh et al 2005, Yeh et al 2006, Ruelle et al 2007, Fagerstedt et al 2014) for the same tree. This is illustrated in Table 1 for the case of sofwoods, with normal wood - comprising opposite wood, lateral wood, juvenile wood, mature wood or flexure wood - clearly distinct from any type of compression wood.

Table 1 Lignin content for different softwood types

Author	Species	Origin	NW	OW	FW	JW	**CW**	**mCW**	**sCW**	**JCW**
Brennan et al 2012	Radiata pine		29	27.6	28.7		**34.8**			
Nanayakkhara et al 2009	Radiata pine	R3+4		27.9				**32.9**	**38.6**	
Nanayakkhara et al 2009	Radiata pine	R10		27.3				**31.4**	**35.4**	
Nanayakkhara et al 2009	Radiata pine	R15+16		27.1				**31.3**	**35.6**	
Nanayakkhara et al 2009	Radiata pine	R1		30			**31.6**			
Nanayakkhara et al 2009	Radiata pine	R2		27.7			**34.9**			
Nanayakkhara et al 2009	Radiata pine	Trunk		27			**37**			
Nanayakkhara et al 2009	Radiata pine	Branch		30.7			**39.6**			
Funda et al 2020	Scot's pine	Trunk	27.6			27.7				
Yeh et al 2005	Loblolly pine	T. Control	29.4							
Yeh et al 2005	Loblolly pine	T. Windy		28.9			**36**			
Yeh et al 2005	Loblolly pine	T. Bent		29.1			**36.6**			
Yeh et al 2006	Loblolly pine	T. Top				29.6				
Yeh et al 2006	Loblolly pine	T. Bottom	27.4			28.5				
Yeh et al 2006	Loblolly pine	T. Middle		28.4		28.6	**37.4**			**37.5**
Mean			28.4	28.3	28.7	28.6	**36.0**	**31.9**	**36.5**	**37.5**

Rx: ring number from pith; T.: trunk
NW: normal wood; OW: opposite wood; FW: flexure wood; JW: juvenile wood
CW: compression wood; mCW: mild compression wood; sCW: severe compression wood;
JCW juvenile compression wood
Bold characters: different lignin content in CW

Three parameters can be adjusted during cell wall thickening to fulfil the biomechanical needs of the tree: final cell wall thickness, orientation of cellulosic reinforcements, chemical composition of cell wall polymers. As a result of this adaptation, variations of physical and mechanical properties can be observed in the wood produced by the tree. In this project, trees from various species and exhibiting active biomechanical movements were selected. Laboratory tests on standard wood specimens sawn from the felled log were related to in-situ residual strain measurements that characterize the biomechanical action of the formed wood, covering as large a range of situations as possible.

Material and methods

Selection of standing trees

Biomechanical studies (Yoshida et al 2000, Jourez et al 2001b, Thibaut et al 2001, Coutand et al 2007, Gril et al 2017) proved that young trees artificially inclined at angles above 20° restore progressively their verticality through the production of reaction wood (RW), either tension wood (TW) on the top or compression wood (CW) on the bottom of the inclined stem. Wood produced on other sides of the stem after inclination, either laterally or opposite, has quite similar features both for anatomy and chemical composition. While restoring verticality, the trees share a common type of bottom geometry with a basal curvature (Clair et al 2006). In natural conditions, accidental inclination of the whole tree by root system rotation due to strong wind or landslide can be observed, mostly for young trees. When these trees restore verticality in the following years they share the same type of bottom geometry (Fig. 1). They

can be considered as natural experiments, and all trees were firstly selected based on this criterion.

To observe a wide diversity of situations, eleven trees were first selected in a tropical rain forest of French Guiana with the help of the botanical expert M.F. Prévost, each from a different family - one tree per species and one species per family. Three poplar trees and three conifer trees (spruce and pines) from temperate forest in France and China were added to the sampling in order to widen the selection (Table 2). For the spruce tree, two logs corresponding to two *GSI* measurement levels (see below) where used, at 1m distance from each other. The mean diameter at breast height of these 17 trees was 26.5 cm.

Table 2 List of trees used in the study

Code	Family	Genus	Species	DBH	RW
1	Melastomataceae	Miconia	fragilis	23.6	GL
2	Meliaceae	Carapa	procera	23.4	GL.
3	Lecythidaceae	Eschweilera	decolorens	23.8	LGL
5	Vochysiaceae	Qualea	rosea	30.3	LGL
7	Cecropiaceae	Cecropia	sciadophylla	25.3	GL
8	Lauraceae	Ocotea	guyanensis	30.9	GL.
9	Flacouritaceae	Laetia	procera	29.4	GLc.
11	Bignonaceae	Jacaranda	copaïa	21.7	NGL
12	Myristiceceae	Virola	surinamensis	20.4	NGL.
14	Cesalpinaceae	Eperua	falcata	27.9	GL.
15	Simaroubaceae	Simaruba	amara	27.7	NGL.
16	Salicaceae	Populus	hybrid	38.3	GL
17	Salicaceae	Populus	hybrid	34.8	GL
18	Salicaceae	Populus	hybrid	25.4	GL
E1	Pinaceae	Picea	abies	24.9	CW
E3	Pinaceae	Picea	abies	24.9	CW
PM	Pinaceae	Pinus	pinaster	20.1	CW
PS	Pinaceae	Pinus	sylvestris	23.0	CW
	Mean			26.4	

DBH: diameter at breast height of the trees in cm

RW, reaction wood type: GL= tension wood (TW) with gelatinous layer, LGL = TW with a lignified G layer, GLc= TW with a multilayer G layer, NGL= TW with no G layer, CW= compression wood

In situ measurements of maturation strain

According to elastic models of residual strain field inside the trunk (Fournier et al 1994a, Fournier et al 1994b), the peripheral longitudinal strain locked in recently formed wood is directly associated to the maturation force just before fibre death (Thibaut 2019). This "maturation strain" α_m is related to the "maturation stress" σ_m by Hooke's law $\sigma_m = MOE^* \alpha_m$, where *MOE* is the modulus of elasticity (MOE) of mature wood in the longitudinal direction. Several techniques exist for in situ estimation of maturation strain at periphery (Yoshida & Okuyama 2002) Clair et al 2013, Yang et al 2005). Here the CIRAD single-hole method was used. Two pins are inserted in the trunk surface in longitudinal alignment at 45mm distance (Jullien 2013). This distance is measured with a linear displacement transducer before and after drilling a hole of diameter 20mm and depth about 20mm in the middle between the two pins. The difference in µm between after and before drilling is called growth stress indicator

(*GSI*); it is positive for a tension force and negative for a compression force. Eight *GSI* measurements are performed on each tree or tree level, equally spaced around the circumference, beginning by the top of the inclined trunk for hardwoods, where tension wood is expected, or by the bottom for softwoods, where compression wood is expected.

GSI is theoretically (Archer 1984) related to maturation strain α by the relationship:

$\alpha_m = \phi * GSI$, α in microstrain ($\mu\varepsilon = 10^{-6}$), *GSI* in µm, ϕ in µε/µm

where the calibration factor ϕ is calculated by modelling the drilling of an anisotropic material occupying a half plane, though a complex equation using wood elastic constants and geometrical factors (distance between pins and hole diameter), see Annex. For various species Baillères (1994) found ϕ values ranging from - 10 to - 15 µε/µm, and Jullien (2013) used - 12.9 µε/µm for beech.

Wood specimens for physical and mechanical properties measurements.

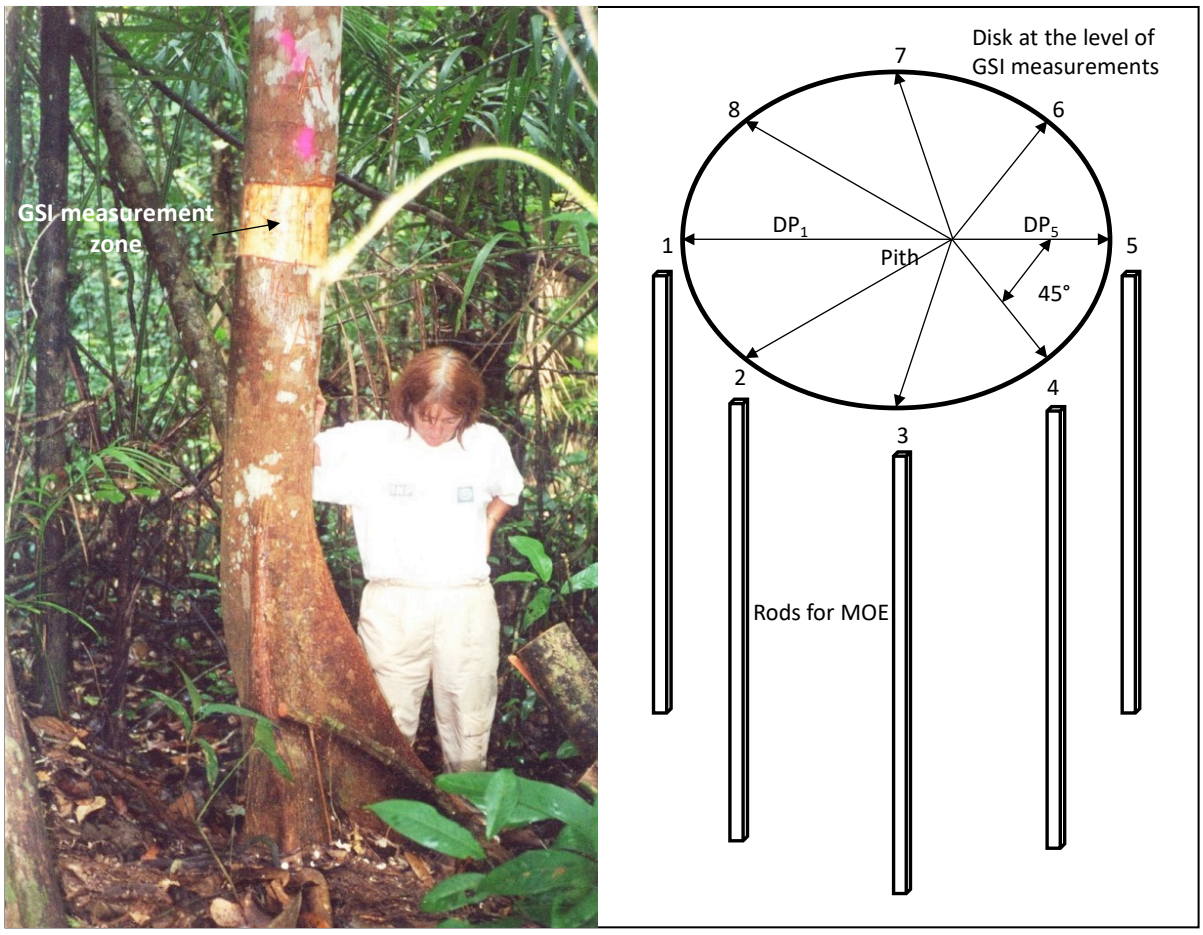

Fig. 1 Tree measured in French Guiana, wooden disk and rods sawn for each tree
DP_x: distance to pith from the x *GSI* point

Just after cutting each tree, a disk (2cm thick) was crosscut at the level of *GSI* measurements (Fig. 1). Distance from pith to bark (DP_x) for each *GSI* measurement position was measured. Eight longitudinally oriented rods where sawn just above the disk, at the 8 *GSI* positions, the closest possible to the bark, few days after tree falling, in CIRAD worksop in Kourou.. The dimensions of the rods were 500mm (L, longitudinal direction) x 25mm (R, radial direction) x 25mm (T, tangential direction) and they were kept in green state, wrapped in food-grade

transparent cellophane**,** until the measurement of green MOE (E_g). A total of 144 rods were prepared.

A smaller rod (50mm x 25 mm x 25 mm) was cut from theses long rods for shrinkage study after E_g measurement.

The remaining long rods (430mm x 25 mm x 25mm) were air dried in the conditioned chamber at 65 % air relative humidity (RH) and 20°C temperature until equilibrium, corresponding to wood moisture content (MC) around 13%. The MOE was again measured on the air-dry rods as such giving a "crude" air-dry MOE. Rods were then planed on four sides to get standard air-dry rods (400mm x 20mm x 20mm) and standard air-dry MOE (E_d) was measured again.

MOE measurements

The flexure free-free vibration method analysed with Timoshenko model (Bordonné 1989, Brancheriau & Baillères 2002) was used for all measurements. Dimensions in the 3 directions (L, R, T) and mass (*M*) of the rods was measured with a good precision (0.1%). The rod was put on 2 thin wires at the first vibration mode positions and tapped at one end, successively on the radial (TL) and tangential (RL) face, corresponding to the RL and TL hitting plane, respectively. The resonant frequency f_i was measured for the three first vibration modes (f_1, f_2, f_3). Using the approximate solution of free vibration theory of Timoshenko, Bordonné (1989) proved that two useful variables x_i and y_i can be built from f_i frequencies, theoretically linked by the expression:

$$y_i = E/\rho - x_i * E/(k*G)$$

where *E* is the axial MOE of the rod (the MOE in L direction), *G* the shear modulus in the hitting plane (G_{TL} or G_{RL}, depending on the orientation of the rod on the wires), ρ the rod density and k a fixed factor. The 3 frequencies (f_1, f_2, f_3) give 3 points of coordinates (x_i, y_i) allowing to fit the equation of a straight line with a regression coefficient that should be very close to 1.0. The slope, the most sensitive to defects, and the intercept of the regression line are $-E/(k*G)$ and E/ρ, respectively. E/ρ is the specific modulus (*SM*) and equals to the square of sound speed in L direction (unit m^2/s^2) while the ratio E/G (E_L/G_{TL} or E_L/G_{RL}) describes elastic anisotropy and is useful for the calculation of ϕ. Density is calculated as mass to volume ratio $\rho = M/(L*R*T)$ and MOE by the formula $E = SM * \rho$. Then *G* can be derived from *E* and *E*/k.*G*, with *k*=5/6 for this geometry (Brancheriau & Baillères 2002).

Basic density and shrinkage measurements.

Wood density depends on wood moisture content (*MC*). Basic density (*BD*), the ratio between anhydrous mass and green volume, is a well-defined parameter characterizing wood honeycomb structure. Wood volume remains constant for green wood until the beginning of drying, while green moisture content (MC_g) can vary widely, typically between 30% and 80%.

Shrinkage behaviour of wood (Glass & Zelinka 2010) is necessary to establish relationships between *BD* and dry density at a given moisture content (12% for example). This shrinkage begins at a reference *MC* called fibre saturation point (*FSP*) and is maximum for anhydrous state (MC_0 = 0%). In order to measure *FSP* and shrinkage rate, the small rod (*L*=50mm x *R*=25mm x *T*=25mm), initially green, is positioned successively in 3 conditioned chambers at decreasing RH (*RH* = 80%, 65%, 30%) and room temperature (*T*=20°C), then finally in an oven at 103°C to obtain the anhydrous state. For each five conditions, mass (M_k) and dimensions L_k, R_k, T_k are measured. The moisture content is calculated as $MC_k = (M_k - M_0) / M_0$ where *k*=0

denote the anhydrous state. The volume is derived from the rod dimension using the formula: $V_k = L_k * R_k * T_k$, and volumetric shrinkage (*VS*) at each moisture content is calculated by the formula: $VS_k = (V_g-V_k)/V_g$. All the points of coordinates (MC_k, VS_k) are aligned along a straight line of equation $y = VS - x * VS/FSP$ (Fig. 2) where *VS* is the total volumetric shrinkage.

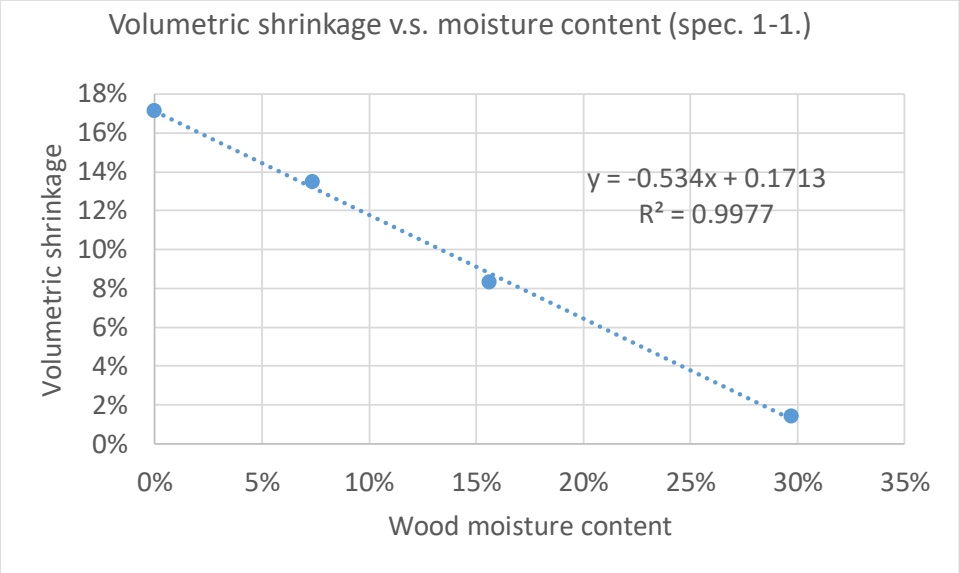

Fig. 2 Measurement of volumetric shrinkage and fibre saturation point

Spec. 1-1.: specimen taken at the first *GSI* position for species Miconia fragilis

The intercepts between this straight line and *y* and *x* axes are the values of *VS* and *FSP*, respectively. The total linear shrinkage in direction L (*LS*) is calculated by the formula: $LS = (L_g-L_0)/L_g$, L_g and L_0 being the length of the rod in green and anhydrous state, respectively.

Results

Relationships between green and dry properties

Because there are more published data on dry than green wood, it is interesting to look at relationships between values of useful properties for tree biomechanics (green state) and wood mechanics (dry state). Concerning the green state, MC_g was on average 89%, ranging from 38% to 182% (39% to 155% as tree average) and was strongly dependant on wood density. The dry state, here, refers to the condition of the specimens after a long storage in a room controlled for temperature (T = 21°C) and air relative humidity (RH = 65%). The corresponding equilibrium MC (MC_d) ranged from 12% to 16% depending on the species and wood type within the species.

For density, green density depending strongly on the seasonal variations of free water content in the xylem, *BD* is mostly used instead. The usual proportional relationship, with a very high coefficient of determination, was observed between *BD* and dry density (*DD*) for this sampling (Fig 3). The proportionality coefficient (*BD*/*DD*) had a mean of 0.826 and ranged from 0.77 to 0.86. It depended mainly on the total volumetric shrinkage (*VS*) (Fig 4).

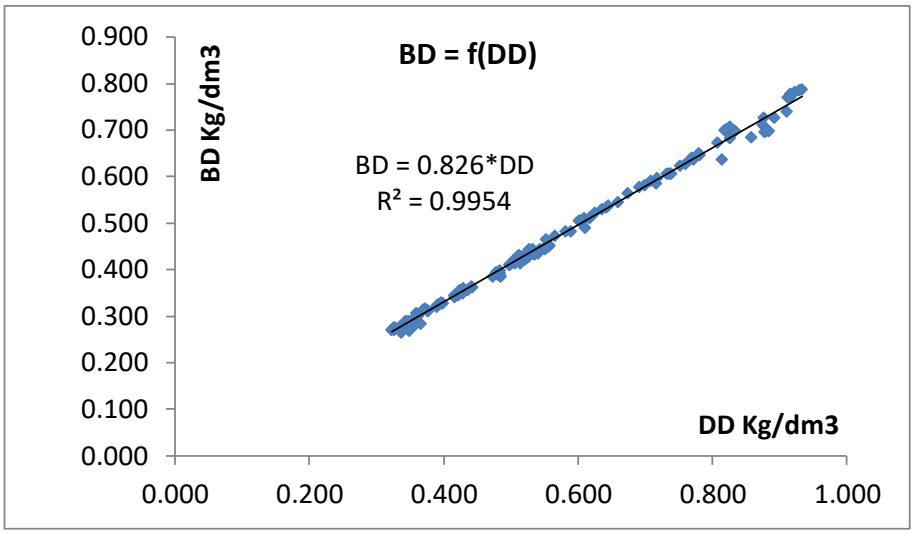

Fig. 3 Proportional relationship between dry and basic density

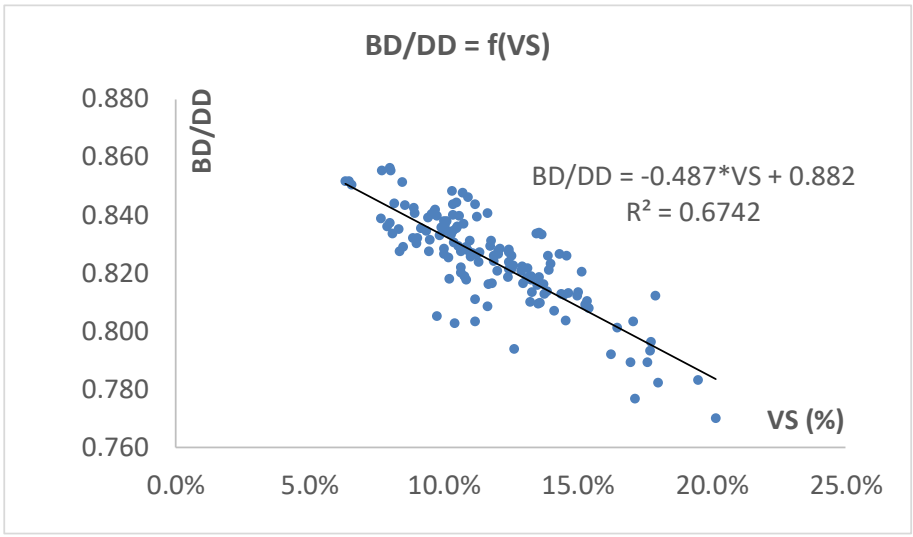

Fig. 4 Dependence of the basic to dry density ratio to the total volumetric shrinkage.

For longitudinal elastic modulus (*E*), specific modulus (*SM*) and shear moduli (G_{TL} and G_{RL}), there is also a proportional relationship between green and dry values. The determination coefficient (R^2) is very high for *E* and *SM* (Fig. 5) and the influence of MC is relatively small (around 10% decrease from dry state).

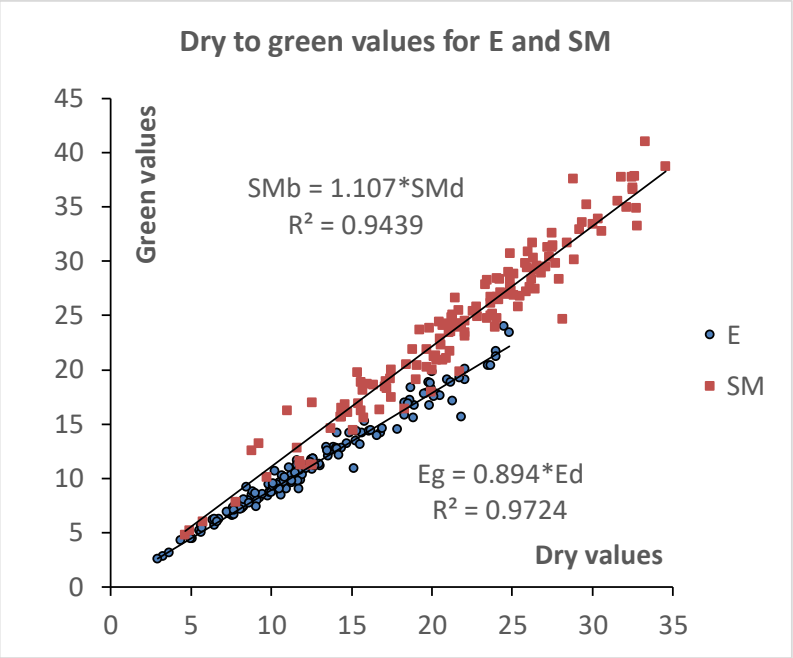

Fig. 5 Proportional relationship between dry and green values for longitudinal MOE (*E*, MPa) and specific modulus (SM, Mm²/s²); *Eg*: green MOE; *Ed*: dry MOE; *SMb*: basic SM; *SMd*: dry SM.

In the case of shear moduli, the proportional relationship is the same for the two directions (TL and RL) with a lower R² mostly due to the much higher sensibility of *E*/*G* (where G stands for either G_{TL} or G_{RL}) to small heterogeneities along the rod (Fig 6). MC influence is more important (around 25% decrease from dry state) but not drastically.

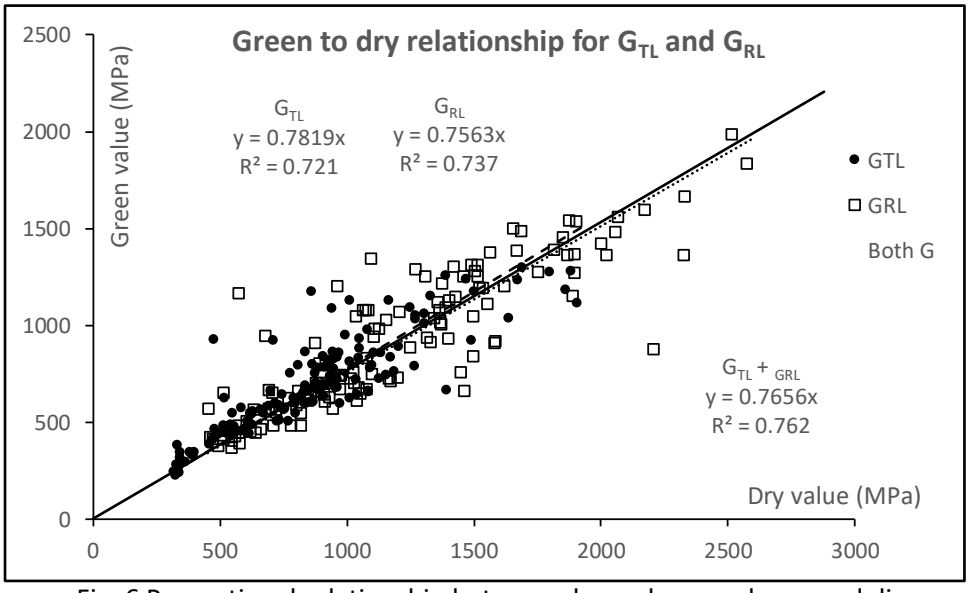

Fig. 6 Proportional relationship between dry and green shear moduli

Estimation of maturation strains and stresses

Using the single hole method to estimate residual strains in an orthotropic material requires the calculation of the conversion parameter ϕ as described in Archer (1984). Baillères in his PhD thesis (1994) used this calculation for 13 different species. Using elastic orthotropic constants coming from statistical models built by Guitard and El Amri (1987), he obtained ϕ values ranging from - 9.1 to - 14.9 με/μm. However, special wood types such as RW were not

considered. Besides, we do not have the 9 elastic constants for the different species and wood types (NW and RW) of this study. From Guitard and El Amri and other literature we have built a data collection of the 6 diagonal moduli (E_L, E_T, E_R, G_{LT}, G_{LR}, G_{TR}) for different species with known densities. We estimated the non-diagonal constants (ν_{LT}, ν_{TL}, ν_{LR}, ν_{RL}, ν_{RT}, ν_{TR}) using Guitard's statistical models and then made the whole calculus of ϕ values for these 96 cases (Excel sheet in annex 1). In order to make that calculus, we have to find the 2 solutions of a second degree equation, which is not possible if the determinant is negative. That happens for a few cases (8 with very low E/G values). There was a very high correlation level between ϕ and the ratio E/G_L and a logarithmic equation gives a very high R^2 (Fig.7). This equation: - ϕ = - 77.57*Ln(E/G) + 34.665 can be used to calculate ϕ with only one anisotropic ratio.

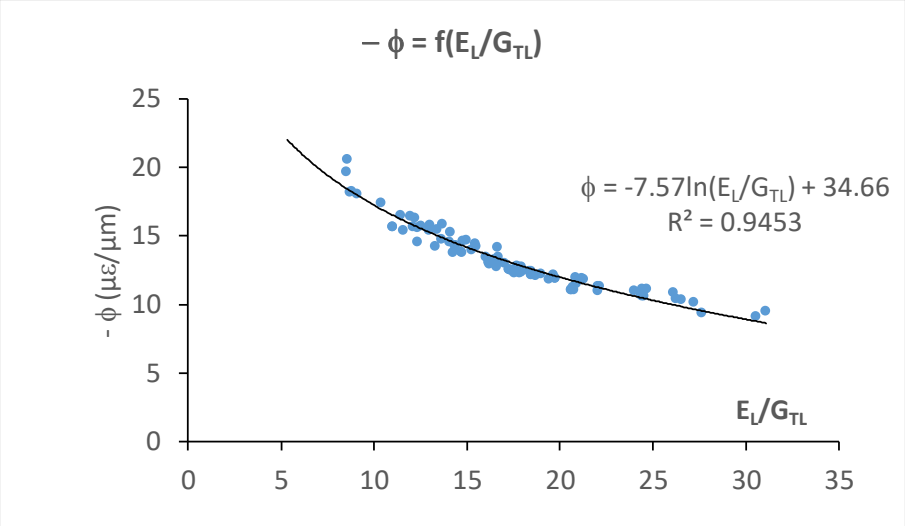

Fig. 7 Relationship between conversion coefficient ϕ and anisotropic ratio (E/G_{TL}).

However, reliable shear moduli data are not always available, so that an alternative method to estimate ϕ is needed. Using the previous formula for the 144 *GSI* measurements, it appears that the calculated ϕ was also very well related (R^2 = 0.81) to the basic specific modulus (*SMb*), the ratio between *Eg* and *BD* (Fig. 8). The higher dispersion around the regression line can be explained by higher uncertainty of *G* measurement as compared to *E.* Finally, this last formula: - ϕ = -0.4811**SMb* + 25.45, was used for all specimens. For the very large range of specific modulus (from 4.6 to 34.6 Mm^2/s^2 for a sampling including RW instead of the usual range between 15 to 30 Mm^2/s^2 corresponding to NW only) the range of ϕ values is rather large, - 5.8 to - 23 με/μm instead of - 9.1 to - 14.9 με/μm in Baillères (1994).

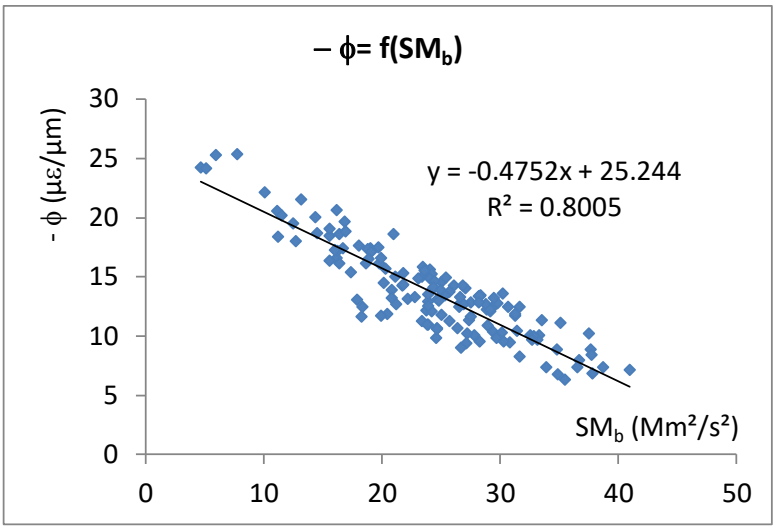

Fig. 8 Relationship between conversion coefficient ϕ and basic specific modulus.
SMb: basic specific modulus (green modulus of elasticity/ basic density) in Mm²/s²

Maturation stress (σ_m) is calculated as the product between maturation strain (α_m) and green longitudinal MOE (E_g). *GSI* being used for studies on tree reaction (Alméras et al 2005b) or biomechanical adaptation to forest density (Jullien et al 2013), the relationship between *GSI* and σ_m was examined at tree level and at population level (our sampling). For each tree there are 8 pairs of *GSI* - σ_m measurements. For all the trees a proportional relationship was found with a very high R^2 level (all R^2>0.97 and 72% of R^2 values >0.99). This result suggests that it is perfectly suitable to use *GSI* as a proxy for tree biomechanics at tree level, the conversion factor $\psi = \sigma_m / GSI$ (in MPa/µm) ranging from 0.064 to 0.259 depending on the species (Table 3).

Table 3 Mean values of parameters per tree

Genus	Species	BD	SMb	Eg	ψ	R^2
Miconia	fragilis	0.71	26.92	19.0	0.232	0.9997
Carapa	procera	0.61	24.87	15.2	0.203	0.9941
Eschweilera	decolorens	0.78	25.92	20.2	0.259	0.9996
Qualea	rosea	0.56	21.29	12.1	0.199	0.9936
Cecropia	sciadophylla	0.35	34.95	12.3	0.107	0.9788
Ocotea	guyanensis	0.46	27.20	12.7	0.156	0.9903
Laetia	procera	0.66	21.97	14.4	0.218	0.9979
Jacaranda	copaïa	0.42	22.14	9.2	0.132	0.9916
Virola	surinamensis	0.29	36.89	10.8	0.084	0.9954
Eperua	falcata	0.70	22.99	16.1	0.234	0.9975
Simaruba	amara	0.30	28.40	8.4	0.096	0.9976
Populus	hybrid	0.29	28.04	8.2	0.110	0.9724
Populus	hybrid	0.34	29.19	9.8	0.114	0.9903
Populus	hybrid	0.38	19.37	7.4	0.128	0.9823
Picea	abies	0.51	20.61	10.0	0.152	0.9933
Picea	abies	0.49	18.10	8.4	0.142	0.9989
Pinus	pinaster	0.42	10.68	11.4	0.064	0.9793
Pinus	sylvestris	0.45	15.88	4.1	0.108	0.9882

BD: basic density (Kg/dm³); *SMb*: basic specific modulus ((Mm²/s²); *Eg*: green elastic modulus (GPa);

ψ: conversion coefficient for maturation stress (in MPa/µm); R^2 regression coefficient of the proportional relationship between σ_m and *GSI* within the tree.

The global relationship between the conversion coefficient and *BD*, for all positions in all trees, shows a very good proportional relationship (R^2=0.97) when rods containing compression wood are excluded (Fig. 9). When no measurement of green elastic modulus is available, basic density can be used to calculate the basic specific modulus and then have a good estimation of the coefficient factor for maturation strain, this simple formula: σ_M=-0.321**BD***GSI* (σ_M in MPa, *BD* in kg/dm^3 and *GSI* in µm) can be used for all cases when there is no compression wood in the measurement zone.

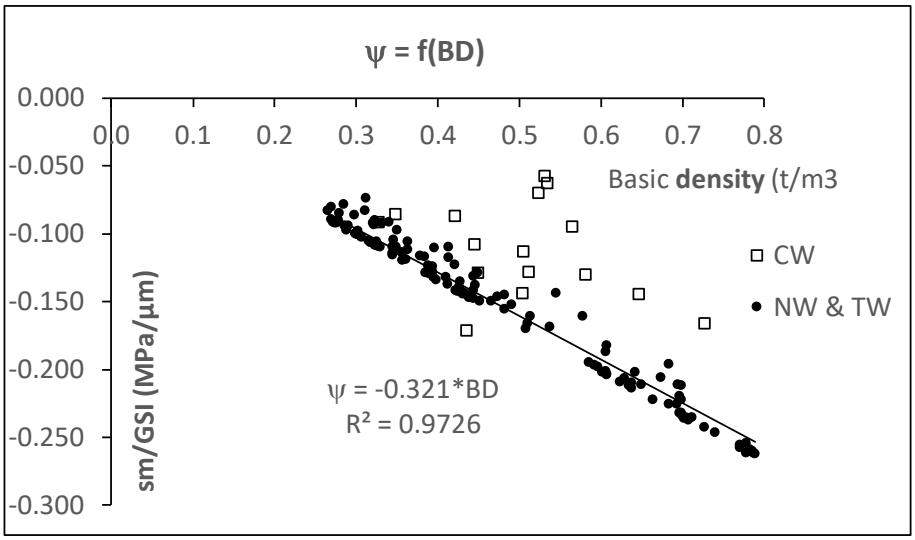

Fig. 9 Relationship between conversion coefficient for maturation stress (ω) and basic density (BD). ψ: conversion coefficient for maturation stress (MPa/µm); BD: basic density (Kg/dm^3); CW: compression wood; NW: normal wood (hardwood & softwood); TW: tension wood

This is not true for positions with compression wood. A very good proportional relationship (R^2=0.89) appears between the conversion coefficient and the modulus of elasticity (Fig. 10), but when the green elastic modulus is available, together with basic density, it is possible to use the conversion coefficient ϕ for maturation strain and then calculate σ_M.

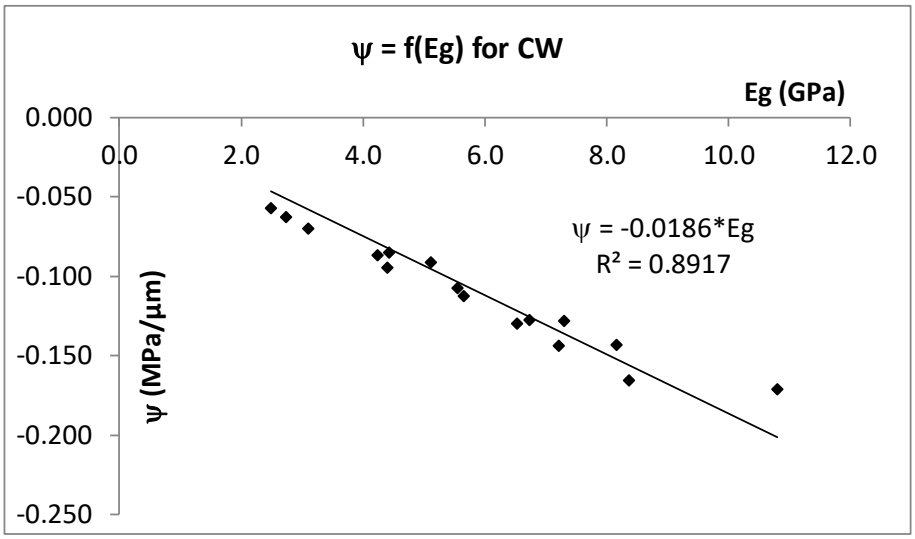

Fig. 10 Relationship between conversion coefficient for maturation stress and green modulus of elasticity, for compression wood

ψ: conversion coefficient for maturation stress (MPa/µm)
Eg: longitudinal modulus of elasticity at green state (GPa)

Force generation and longitudinal wood properties

The maturation stress σ_m is the force created by the living wood per unit surface. It is the product of the maturation strain (α_m) and the green L MOE (E_g), itself the product of basic density (*BD*) and basic specific modulus (SM_b). *BD*, SM_b and α_m are the parameters resulting from the activity of the living wood until fibre death.

A correlation analysis (Table 4) shows that σ_m is mostly dependant on α_m (R^2=88%) then on SM_b (22%) and on *BD* (8%). Moreover, the three parameters *SMb*, E_g/G_{TLg}, E_g/G_{RLg} are very strongly correlated. They are all indicators of wood anisotropy. Correlation coefficients between *LS* and α_m is weak, although it is known that RWs have strongly different values for this property (Jourez et al 2001a, Gardiner et al 2014).

Table 4: Correlation (Spearman) coefficients between parameters.

	αm	σm	BD	SMb	LS(%)	Eg	$G_{TL}g$	$G_{RL}g$	$E_L/G_{TL}g$	$E_L/G_{RL}g$
αm	**1**	**0.941**	0.095	**0.381**	0.196	**0.435**	-0.049	-0.047	**0.431**	**0.422**
σm	***	**1**	**0.290**	**0.467**	0.137	**0.685**	0.059	0.058	**0.559**	**0.495**
BD		***	**1**	**-0.346**	0.196	**0.593**	**0.790**	**0.783**	-0.094	-0.178
SMb	***	***	***	**1**	-0.189	**0.500**	**-0.499**	**-0.508**	**0.843**	**0.828**
LS(%)	*		*	*	**1**	-0.074	0.271	0.277	-0.231	-0.175
Eg	***	***	***	***		**1**	**0.289**	0.255	**0.619**	**0.534**
$G_{TL}g$			***	***	**	***	**1**	**0.866**	**-0.516**	**-0.473**
$G_{RL}g$			***	***	**	**	***	**1**	**-0.421**	**-0.587**
$E_L/G_{TL}g$	***	***		***	**	***	***	***	**1**	**0.877**
$E_L/G_{RL}g$	***	***	*	***	*	***	***	***	***	**1**

Bold characters: correlation significant at 0.001
***: correlation significant at 0.001 **: correlation significant at 0.01
*: correlation significant at 0.05
α_m: maturation strain in micro-deformation; σ_m: maturation stress in MPa
ϕ and ψ: conversion coefficients between *GSI* and maturation strain and stress, respectively
BD: basic density (anhydrous mass/green volume) in kg/dm^3
LS: total longitudinal shrinkage
E_g: green longitudinal elastic modulus
G_{TLg} and G_{RLg}: green TL and RL shear modulus, respectively
SMb: basic specific modulus (green longitudinal elastic modulus/basic density) in Mm²/s²
E_g/G_{TLg} and E_g/G_{RLg}: anisotropy ratio in the green state respectively in TL and RL case

Visual observation of the wood disks (Fig 11) allowed affecting a wood type to each tested specimen: 1=CW, 2=both CW and NW, 3=NW, 4=both NW and TW, 5=TW. Wood types 2 and 4 were attributed to rods containing both RW and NW. Transverse sections 15µm thick were cut from two NW and two TW rods (in the middle of the rod) in order to examine wood anatomy (Fig. 12 and Fig.13).

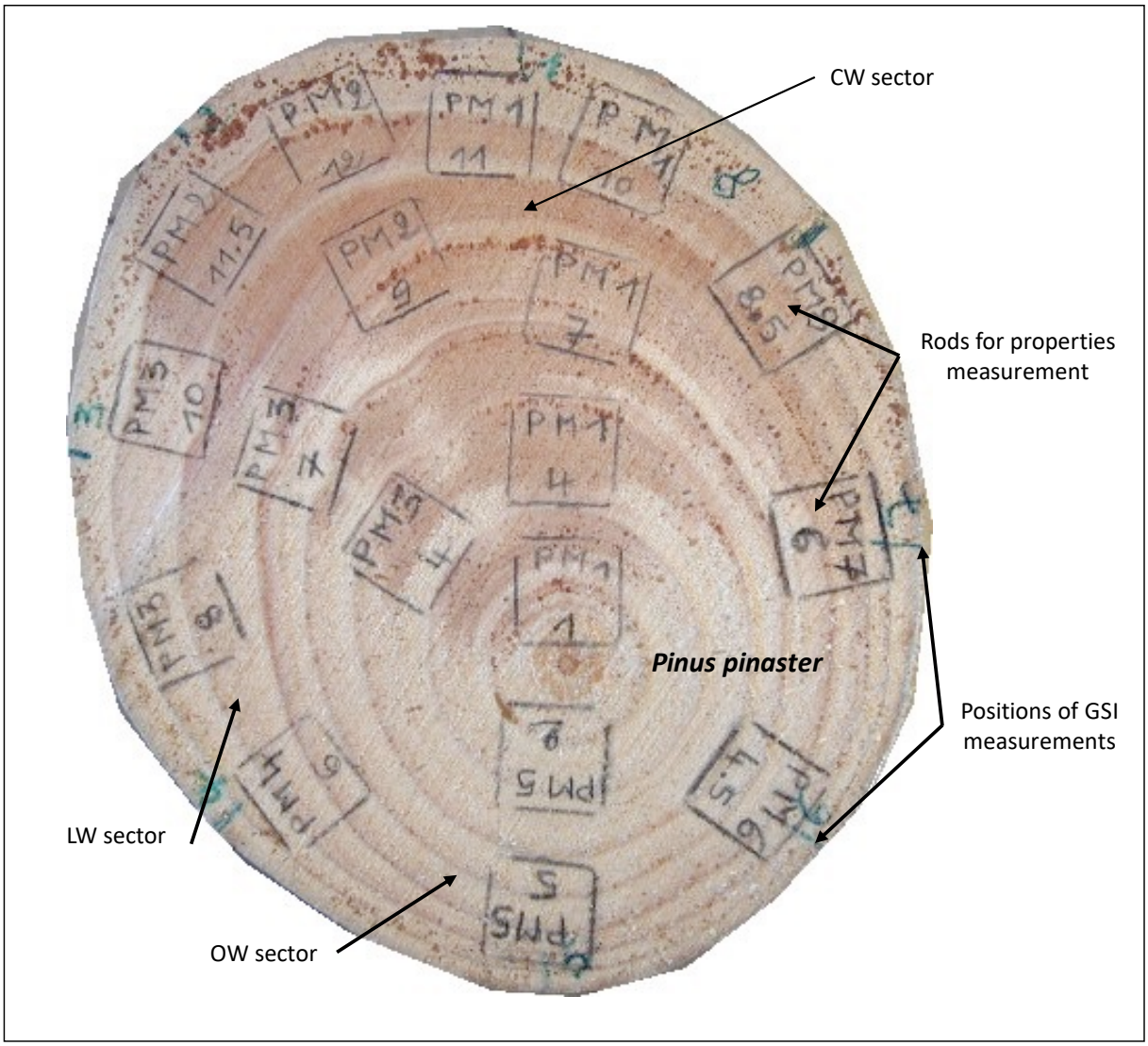

Fig. 11 Image of the section of *Pinus pinaster* tree with the positions of measurements
CW: compression wood, OW: opposite wood, LW lateral wood
The tree is young hence all wood can be considered as juvenile wood (JW)

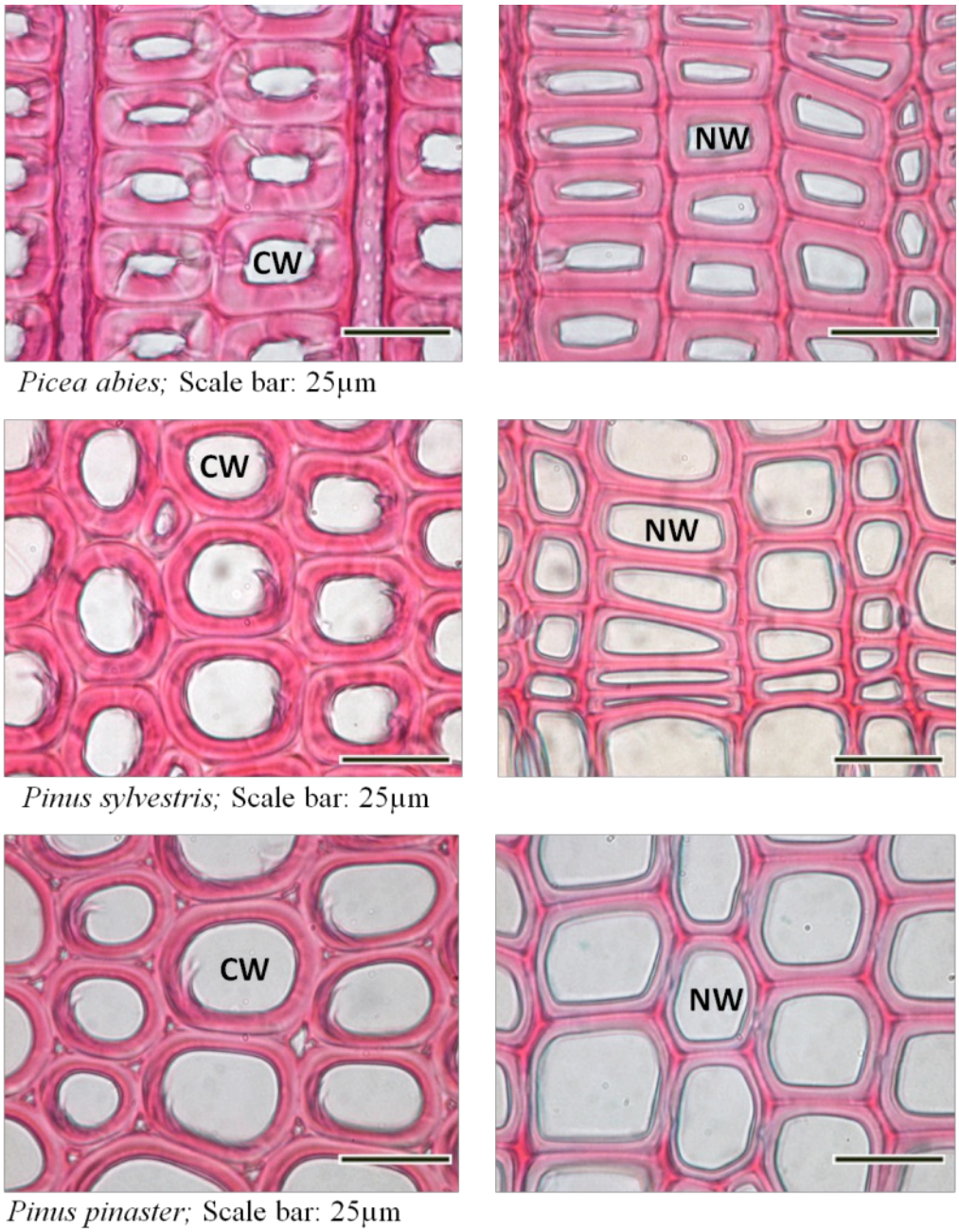

Fig. 12 Comparative anatomy of compression wood and normal wood for the conifer species
NW: normal wood; CW: compression wood

For conifers, the difference between CW and NW is classical (Ruelle 2014). The mean microfibrillar angle (*MFA*) is always high for CW, and globaly lower for NW but with some overlap around 30-35° (Brémaud et al 2013). The trees were rather young (Fig. 11) so most of the NW can be considered as juvenile wood (JW).

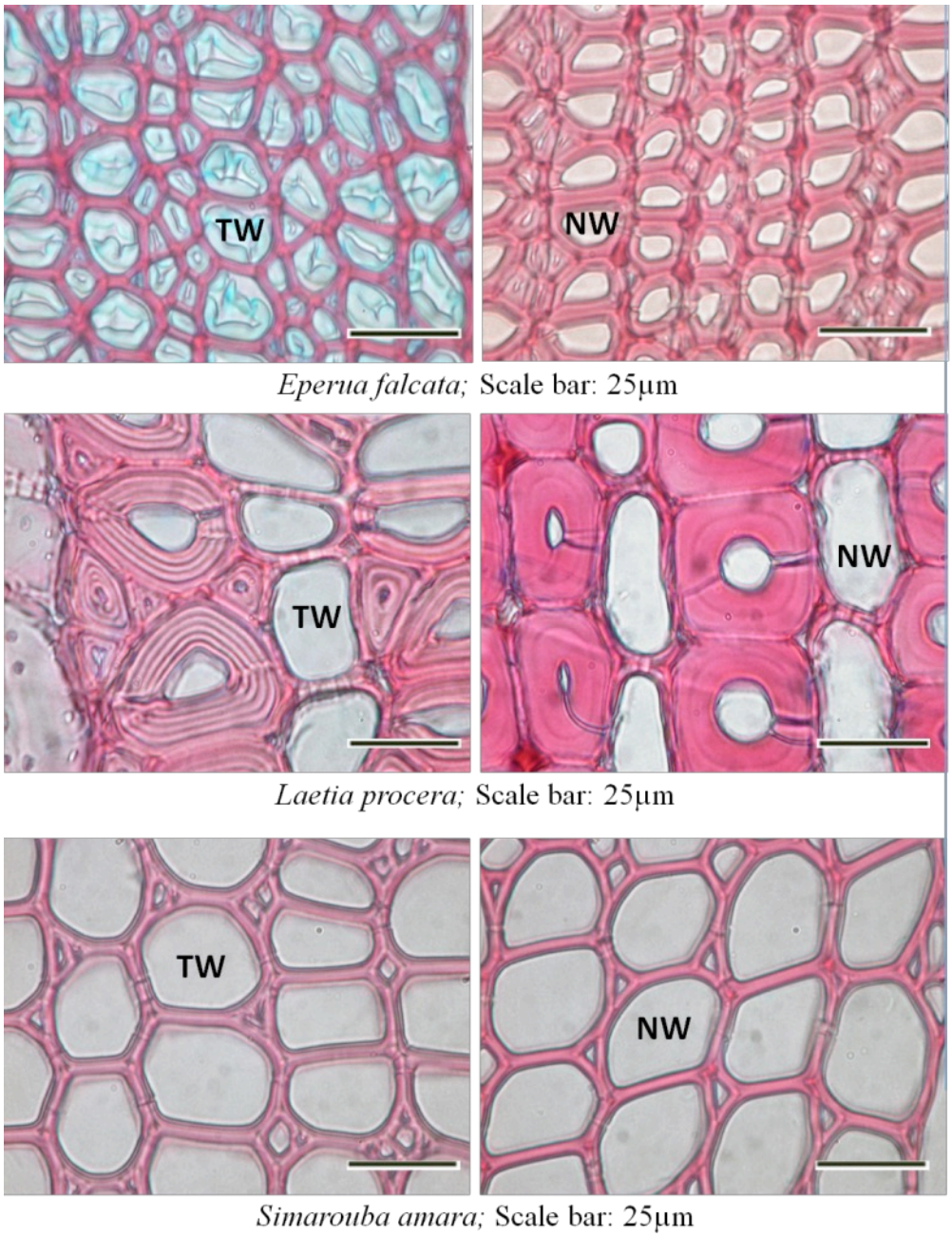

Fig.13 Comparative anatomy of tension wood and normal wood for three tropical species
NW: normal wood; TW: tension wood

For hardwoods, a majority of G-layer type TW (3 poplars, Miconia, Carapa, Ocotea, Cecropia, Eperua) were studied (Table 2), two species had a lignified G layer (Eschweilera & Qualea), one a peculiar multi-layered G layer (Laetia) and three no G layer fibre (Jacaranda, Virola, Simarouba), according to a recent classification based on 242 tropical species (Ghislain et al 2019). Measurement of *MFA* on the 3 species represented in Fig. 13 (Ruelle et al 2007) showed lower values for TW (2° to 14°) than for NW (10° to 35°), with some overlap around 10°-14° .

The clear distinction between wood types for the parameters describing force generation (Fig. 14) results from the very definition of RW as force generator: compression (negative strain/stress) for CW, slight tension for NW, high tension for TW. Median maturation strain is very high, around 2200 µdef (0.22%) in absolute value for both RWs, much lower (620 µdef) for NW. Median maturation stresses are not so different, in absolute value, between CW (-9.5

MPa, compression) and NW (+6.6 MPa, tension), due to the low value of elastic modulus (median 5.5 GPa) for CW (10.2 GPa for NW). The difference increases a little for TW (+31 MPa, tension) due to the higher median value of elastic modulus (14.5 Gpa), so tensile stress is nearly 5 times higher in TW as compared to NW. For a small new ring portion of 100mm² (50 mm wide, 2mm thick) the force created in CW (around 1 KN) or TW (around 3 KN) sectors are very high.

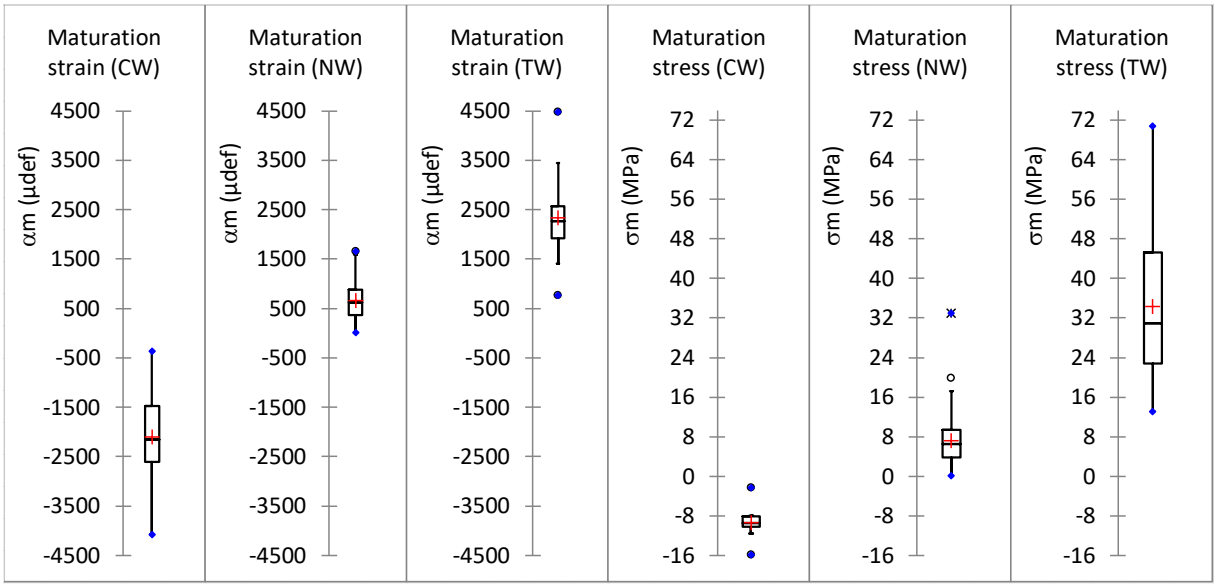

Fig. 14 Distribution of maturation strain and stress values for different wood types
α_m: maturation strain in micro-deformation; σ_m: maturation stress in MPa
CW: compression wood; NW: normal wood; TW: tension wood

The parallel regular progression of values for anisotropy factor shown in Fig 15, reflects the fact that the *MFA* decreases from CW (up to 50°) to TW (near to 0°), with, however, a large overlap between NW and TW and a smaller one between NW and CW. This is not true for *LS* (Fig. 15 and Fig. 16): both RWs have a high *LS* while NW keeps a very low *LS* level (less than 0.4%).

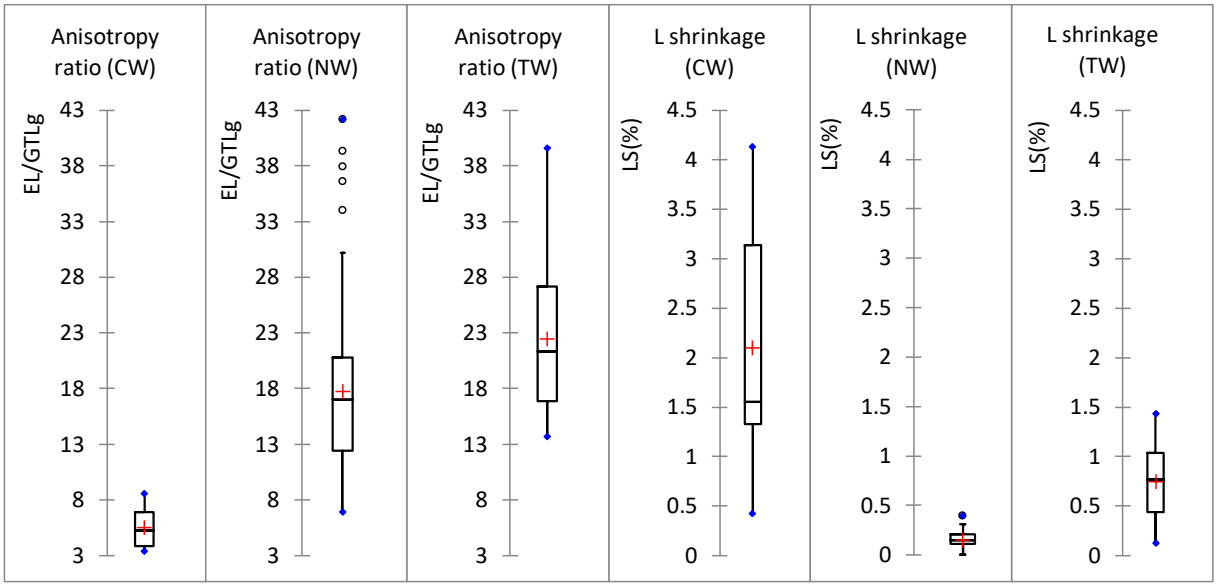

Fig. 15 Distribution of L shrinkage (*LS*) and anisotropy ratio (E/G_{TL}) for different wood types

LS: longitudinal shrinkage, E_g/G_{TLg}: anisotropy ratio at green state.
same legend as Fig. 11

The relationship between *LS* and α_m (Fig. 16), α_m and *SMb* (Fig. 17) or *LS* and *SMb* (Fig. 18) evidences different patterns for NW, CW and TW. It should be noted that α_m and green wood properties (*LS* and *SMb*) are not strictly measured on the same material and this contributes to lower correlations between them.

LS grows with the absolute value of α_m (Fig. 16) for both CW and GL-TW while *LS* keeps low for all the NWs.

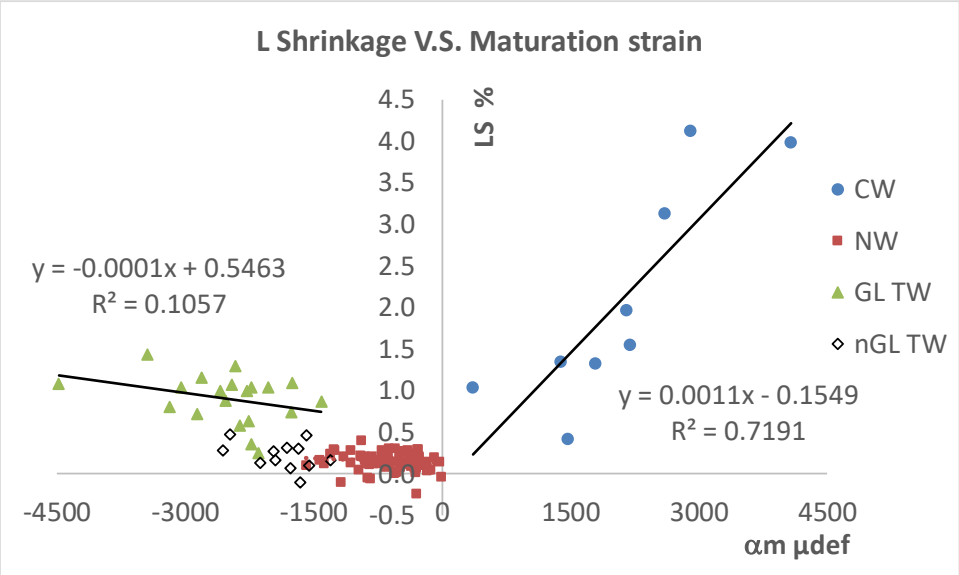

Fig. 16 Evolution of longitudinal shrinkage with maturation strain
CW: compression wood
NW: normal wood for both softwoods and hardwoods (no significant difference)
GL-TW: tension wood with gelatinous layer
nGL-TW: tension wood without gelatinous layer
α_m: maturation strain; µdef: micro deformation (10^{-6})

There is no evident influence of α_m on *SMb* (Fig.17) for NW while *SMb* increases when α_m decreases in absolute value for both TW and CW.

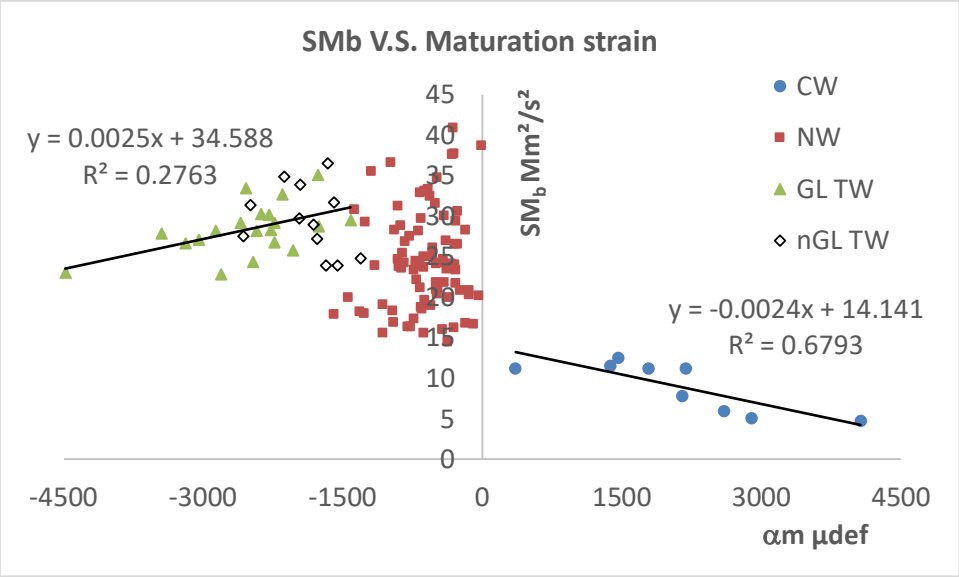

Fig. 17 Evolution of longitudinal maturation strain with wood elastic anisotropy
Same legend as Fig. 16
SMb: basic specific modulus (green modulus/basic density)

LS and *SMb* are measured on the same rod so the uncertainties are lower. For all wood types *LS* decreases significantly when *SMb* increases (Fig. 18) but the evolution is rather steep or very steep for TW and CW while it is smooth for all NWs. It should be noted that the TW of species without G layer is similar to NW for this relationship. High L shrinkage is mostly present when there is a G layer in the TW fibre.

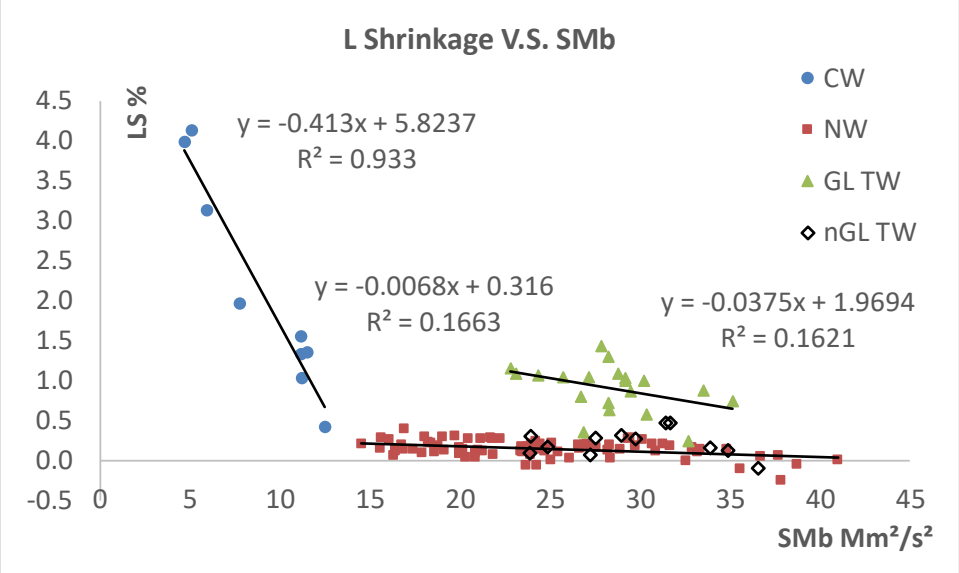

Fig. 18 Evolution of longitudinal shrinkage with wood elastic anisotropy
Same legend as Fig. 16 & 17

Discussion

Green to dry wood properties

BD is now commonly used in ecological studies on carbon sequestration in forests. Using the large CIRAD database (4022 trees) a very nice proportional relationship was found between *DD* (12% moisture content) and *BD* with a proportional factor of 0.828 (Vieilledent et al 2018).

Here, with a quite different sampling, a factor of 0.826 was obtained. The very large range of *VS* due to the presence of CW shows that this proportional factor ranges from 0.78 to 0.86 (Fig. 4) with a good prediction of the variation by *VS* which can be easily measured at the same time as BD.

In our study, elastic properties are measured by vibration technique, namely high deformation rate where little viscosity is active (no creep added to the instantaneous elastic strain). The decrease between dry and green state is only around 10% for *E* and around 25% for *G*, either G_{RL} or G_{TL}. The Wood Handbook (Gretschman 2010) gives MOE values in the green state and at 12% MC, as means for 64 hardwood species and 37 softwood species, using different rods for each condition in order to measure also rupture strength. A very good proportional relationship is also obtained (R^2=0.86 for hardwoods, R^2= 0.95 for softwoods), as compared to R^2=0.97 in this study. The decrease between air-dry and green states is around 20% (22% for hardwoods, 20% for softwoods), which is significantly different (two times greater). A small part of the difference can be explained by a different equilibrium MC (from 12% to 16% for air-dry wood in this study), but the greatest part is likely to originate from the experimental method. In the Wood Handbook the measurements are performed in 3 points bending at slow deformation rate, allowing some initial creep which is more important for green wood than for dry wood.

GSI as a good indicator for growth stresses

The single hole method has the advantage of being quick, easily operable in all field situations and cheap, making it most appropriate for large measurement campaigns such as the "Stresses in beech" EU project where 8,000 *GSI* data were collected in situ (Jullien et al 2013). It requires, however, the use of a conversion factor (ϕ) from *GSI* to α_m. The theoretical computation of ϕ, based on an orthotropic elastic model of residual stress (Archer 1984), depends of wood anisotropy near the measurement zone and thus depends on the wood species as well as the wood type. It can be practically estimated from the basic specific modulus (SM_b) that ranges from 5 Mm^2/s^2 for severe compression wood to up to 40 Mm^2/s^2 for resonance wood with high sound speed. The range of resulting maturation strains found in this study is very similar to values in the literature for CW (Yamamoto et al 1991, Huang et al 2001, Yamashita et al 2007) and TW (Yoshida et al 2000, Fang et al 2008, Clair et al 2013), around -4000 to +4000 µdef.

The 8 maturation stresses calculated for each tested tree were proportional to GSI values with very high regression coefficients (R^2>0.97), so it is possible to use *GSI* as a proxy of growth stress within a tree, even when it contains severe CW or TW sectors. Furthermore, the conversion coefficient ψ between *GSI* and maturation stress is proportional to BD with a very good regression coefficient (R^2=0.97), except in the case of CW occurrence. This means that for hardwoods, *BD* is the only parameter needed for the conversion coefficient ψ.

Strain, stress and force generation.

Force generation is one of the functions provided by fibres/tracheids during cell-wall thickening, and force asymmetry between both sides of a wooden axis is the motor of its posture control (Alméras et al 2005b, Alméras et al 2009). The force (*F*) produced by an angular portion of new living xylem equals the product of the area (*A*) of that portion, orthogonal to the force, by the maturation stress (σ_m) generated in the xylem tissue during cell-wall thickening: $F=A.\sigma_m$. *A* depends both on the amount of cell division in the cambium and on the cell expansion until the end of primary wall setting (Cuny et al 2012). σ_m is also the

residual stress present in the last ring of sapwood after the programmed fibre death, and can be measured in situ by classical residual stress measurement methods. The existence of this pre-stress enhances the flexure resistance of wooden axes (Gril et al 2017) and thus contributes to the skeleton function of wood in the tree.

Maturation stress σ_m is associated to maturation strain α_m via Hooke's law: $\sigma_m = E.\alpha_m$, where E stands here for E_g, the MOE of xylem tissue at the end of the maturation process. α_m is locked in the wood until stress release, e.g. by cutting. It is largely agreed that α_m, as a result of the whole lignification process, is the source of σ_m. As the new layer is glued on a solid rigid core, the "natural" extension or shrinkage of the fibre cannot be expressed, resulting in stress occurrence.

This longitudinal expansion during secondary wall deposition is of the order of 0.1%, much smaller than the expansion occurring during primary wall building. But, at the end of the maturation process, the MOE of a xylem portion is very high, of the order of 10 GPa, thousands of time bigger than the modulus at the end of primary wall expansion. As a result, maturation stresses have high values allowing to produce large forces (of the order of kN) and large motor actions (Alméras et al 2005b).

In the L direction, thanks to the honeycomb-like microstructure of wood with a quasi-parallel alignment of the wall of fibres or tracheids, wood MOE (E) is directly related to cell-wall MOE (E_w). Below *FSP*, when cell cavities (lumens) contain only air and water vapour, wood specific modulus $SM=E/d$ equals that of the cell-wall $SM_w=E_w/d_w$, where d_w is the cell-wall density; both being equal to the square of the longitudinal sound of speed (Gibson and Ashby 1999). Wood MOE can thus be expressed as: $E = d \times SM = d \times SM_w = (d/d_w) \times E_w$. In this expression the relative density (d/d_w) represents the cell-wall proportion; it is a basic property of the cellular material, while E_w is a basic property of the cell wall. Both d_w and E_w depend on the properties of the polymers composing the cell wall; while d_w variation is very small among wood species and types (d_w ~ 1.5g/cm^3), E_w is highly dependent on the ultrastructural organisation of the cell wall such as the orientation of cellulosic microfibrils. The longitudinal maturation strain α_m, like E_w, depends on cell-wall composition and organization.

Wood formation involves three successive processes: cell division, expansion and maturation: the number of cells produced during a given period of time is controlled by cell division, their size by cellular expansion and the properties of their wall by cellular maturation (taken here in a broad sense, including the cell-wall thickening). Wood relative density (d/d_w), approximately proportional to the ratio between cell-wall thickness and cell diameter, is controlled both by division and by maturation, while cell-wall MOE (E_w) and maturation strain (α_m) are mostly controlled by maturation. Wood MOE (E), as the product of E_w and d/d_w, and maturation stress σ_m, as the product of E and α_m, are both controlled by expansion and maturation. When a layer of wood is deposited at stem periphery, the force produced by a portion of that ring, equal to the product of σ_m and the ring thickness, is controlled by expansion and maturation, and by division - and so is the bending motor force produced at the stem level, since it amounts, roughly, to the product of the driving forces on the two opposite faces and the total diameter growth. The regulation of such a scheme is very complex and is far from being fully understood today. Anyway, this regulation of forces is also, at the end, a regulation of all wood properties because it affects chemistry, anatomy, and cell-wall ultrastructure.

Compression wood, normal wood and tension wood

It is natural and useful to use maturation strain α_m as basic indicator of maturation because it depends only on this living phase, but it is also the case of E_w as well as of longitudinal shrinkage (*LS*), which depend essentially only the composition and structure of the cell wall. Hence the relationships between these three parameters can provide information on what happened during secondary wall thickening until programmed cell death.

The distinction between wood types is based on α_m: CW produces positive α_m, TW very large negative α_m and NW very low to rather high negative α_m. All have a muscular action for the control of stem curvature: NW alone for a moderate action, or combined with RW (either CW or TW) for a strong action. Many papers highlight that triggering RW mobilise specific genes (Gardiner et al 2014) and changes strongly the chemical composition of the cell wall matrix as compared to NW. This is probably what explains the different patterns in the relationships observed in Fig. 15, 16 & 17.

For NW, no significant difference seems to exist between softwoods and hardwoods in spite of chemical differences in chemical composition of the matrix, mainly for the hemicelluloses (Gérard et al 2020). For all NWs there is a wide range of *MFA*, and consequently, in specific modulus (Fig. 14), with a large range overlap for TW and a small one for CW (Brémaud et al 2013, Ruelle et al 2007). But no significant relationship was fond between α_m and *SMb* (Fig. 17) although both have large variations. Many papers have described a very significant relationship between *MFA* and α_m but they combine NW and RW and the significance comes from the RW (Yamamoto et al 1991, Okuyama et al 1994, Yamamoto et al 1998).

For CW there is a strong relationship between α_m and *SMb*; this is similar to all results from the literature and is consistent with models built on the assumption of a bulk shrinkage of cell wall matrix (Alméras et al 2005a, Yamamoto et al 1988, Guitard et al 1999). The models cannot be well adjusted to both NW and CW.

For TW although it is admitted that *MFA* is always small or very small, the specific modulus is not as high as for NW with low *MFA*. A tiny tendency of lower SM_b for higher maturation strain (in absolute value) seems to appear for G-layer TW. *MFA* cannot explain the high maturation strain of TW, and there is no clear difference between G-layer, lignified G-layer and no G-layer types of TW regarding the relationship between *SMb* and α_m.

One clear indication within each tree is the much higher *LS* for both RWs as compared to the NW in the same tree (Table 5). But this difference is higher in the case of G-layer TW.

Table 5 Differences between normal and reaction wood

Type	αm NW	**αm RW**	**RW/**NW	LS NW	**LS RW**	**RW/**NW	SMb NW	**SMb RW**	**RW/**NW
SW	386	**-2103**	**-5.4**	0.15	**2.10**	**14.4**	21.08	**9.01**	**0.43**
HW GL	796	**2255**	**2.8**	0.17	**0.89**	**5.3**	25.48	**28.42**	**1.12**
HW GLc	522	**3579**	**6.9**	0.15	**1.22**	**7.9**	19.16	**24.58**	**1.28**
HW LGL	668	**2174**	**3.3**	0.17	**0.53**	**3.0**	22.95	**29.21**	**1.27**
HW NGL	637	**1995**	**3.1**	0.11	**0.31**	**2.9**	27.89	**32.18**	**1.15**

SW: Softwood; HW: hardwood; NW: normal wood; RW: reaction wood
GL: gelatinous layer; GLc: multi-layered GL; LGL: lignified GL; NGL: no GL
α_m: maturation strain; *LS*: longitudinal shrinkage; *SMb*: basic specific modulus
RW/NW: ratio between RW and NW values

For conifers, the difference of dependence between *LS* and *SM* for NW and RW was described before (Watanabe & Norimoto 1996).

Models for longitudinal shrinkage of wood (Cave 1972, Yamamoto et al 2001) predict a steady growth of *LS* with growing *MFA* over 30° and suggest a small inverse situation for small *MFA* below 30°. Remembering that specific modulus is strongly decreasing (from 30 to 10 Mm^2/s^2) when *MFA* increases from 10 to 30° (Cowdrey & Preston 1966, Cave & Hutt 1968, Brémaud et al 2013), *LS* should increase when SM_b increases in the range 11 to 33 Mm^2/s^2 (using the conversion factor 1.1 between dry specific modulus and SM_b). In fact, there was a very significant negative correlation between *LS* and SM_b for NW in that range. The same seems to be true also for TW, but SM_b was supposed to be higher for the low *MFA* values in TW. Moreover, G-layer TW has a much higher *LS* than NW for similar values of SM_b.

The paradoxical situation of longitudinal shrinkage for G-layer tension wood was described in the literature (Dadswell & Wardrop 1955, Jourez et al 2003, Clair & Thibaut 2014). Many recent papers discuss the role of cellulose nano-fibres organisation within the microfibrils, using both experiments and models (Clair et al 2008, Chang et al 2015, Alméras & Clair 2016, Gorshkova et al 2018). α_m and *LS* are considered but these models and could be also efficient to predict the specific modulus "anomaly" for G-fibres.

Trade-off between active posture control and passive pre-stressing

The tensile pre-stressing of stem periphery enhances its flexure resistance, thanks to the resistance in tension of wood being typically twice that in compression (Gordon 1978, Thibaut & Gril 2003, Moulia et al 2006). In order to roughly quantify this, the relationship between resistance to compression (*CR*) and basic density (*BD*) was examined on the data for green wood in the wood handbook (Kretschmann 2010). *CR* can be predicted by a proportional formula: $CR = k*BD$, where $k = 52.5$ for softwoods and 46.1 for hardwoods with *CR* in MPa and *BD* in kg/dm3. The specific resistance to compression (resistance/density) is rather unaffected by microfibril angle (Gindl 2001, Gindl & Teischinger 2002), specifically for CW (Pillow & Luxford 1937, Cockrell & Knudson 1973), and the same ratio can be used for CW and NW.

The same database gives also values of green flexure resistance (*MOR*), roughly twice *CR*, that can be used as a conservative value for tensile strength (Kretschmann 2010); green wood MOR also can be predicted by a proportional formula: $MOR = k*BD$, where $k = 108$ for both softwoods and hardwoods. According to a smaller database (18 species), associated to the large wood handbook database, the green ultimate tensile resistance is in average 60% higher than green *MOR* for the same species (Markwardt & Wilson 1935). Published data of green TW resistance are scarce. Clarke (1937) writes that tensile strength of TW is 10% higher than that of NW for beech, while compression strength of TW is much lower, which is consistent with the higher proportion of cellulose microfibrils in TW. It can also be accepted that green tensile strength of TW is around 60% higher than its green *MOR*.

The crude approximation of *CR* and *MOR* in the green state, based on *BD*, was used for all tested rods. Table 6 summarizes, for NW, TW and CW, the mean values of *BD*, *CR* and *MOR*, together with the maturation stress σ_m. According to the pre-stressing represented by σ_m, in case of tree bending the maximum allowable compressive stress case is equal to the sum of *CR* and σ_m, while the maximum allowable tensile stress is the difference between *MOR* and σ_m.

Table 6 Pre-stressing and flexure resistance for different wood types

Tree	BD	DPrel	Eg	CR	MOR	σm	σm + CR	MOR-σm
mean CW	0.56	1.26	5.1	29.5	60.8	-9.3	**20.2**	70.1
mean NW SW	0.46	0.91	10.9	22.4	46.3	3.8	26.2	42.5
mean NW HW	0.47	0.93	11.4	21.7	50.9	8.1	29.7	42.8
mean TW	0.51	1.16	14.4	23.3	54.8	34.3	57.6	**20.5**

BD: basic density (Kg/dm^3); *Eg*: green modulus of elasticity (GPa);
DPrel: ratio between rod distance to pith (*DP*) and mean *DP* for the 8 rods of the tree;
CR: longitudinal crushing resistance (MPa); *MOR*: flexure resistance (MPa)
CW: compression wood; NW SW: normal wood of softwood; NW HW normal wood of hardwood;
σ_m: maturation stress or pre-stress (MPa)

For a well-balanced tree containing no RW, σ_m is always positive (tension) on both sides of the trunk under wind action, and the wind stress is maximum and the same in absolute value, on the two faces: compression downwind, tension upwind. If the maximum wind stress is around 25 MPa for the mean trees of Table 6, the NW will be safe in all wind situations. But for both types of RW the allowable resistance to compression (case of CW) or to tension (case of TW) are similar and lower than a wind stress of 25MPa. Stresses due to strong reacting forces may bring danger in case of wind action either on the compressed side for softwoods or the tensile side for hardwoods.

As *MOR* is likely to be much lower than tensile strength, the situation may not be critical for a TW side, but for the higher tensile stresses there may be a small wind stress attenuation by ovalisation of the cross section inducing a growth of the second moment of inertia in the wind direction.

The compressive stress produced by CW is obviously dangerous in case of strong wind opposite to the CW side. The trade-off between pre-stressing of the skeleton and high force asymmetry for verticality restoration is managed in a rather sophisticated way as can be examined on Fig. 11 and Table 6. For CW, density is higher, MOE is much lower and ring width is much higher - with ovalisation of the cross section. A high compressive force in the newly formed CW is achieved, despite the very low MOE, by higher density and much higher ring width. *CR* is higher due to higher density and maturation compressive stress is limited by the small value of MOE so that the maximum allowable compression stress is not so low. Moreover, there is a large heterogeneity of MOE within the cross section between CW zone and the rest. The neutral axis in bending under wind action will no more be in the geometric centre of the section. As a result, the strain level at periphery will be 15 to 20% higher in the low modulus portion (the compression wood side) and lower in the other side. As MOE is much lower in the CW side (2 times lower), the compressive wind stress will be lower than expected for a normal tree. Ovalisation of the cross section will bring a small additive security factor and the sum of these compensations should be enough for wind safety in such a case.

Conclusion

The combined growth stress evaluation on standing trees and laboratory measurements of wood properties on a large range of situations (different species and densities, NW and RW) bring useful tools for this kind of studies. 1- very good proportional relationships were established for the relationship between green and dry state for density, specific modulus,

longitudinal elastic (MOE) and shearing modulus of elasticity (G_{TL} and G_{RL}). Hence dry wood properties can be used whether there are no green wood data. 2 - a simple conversion coefficient (ϕ) was obtained between growth stress indicator (*GSI*) coming from the single hole method and maturation strain using the basic specific modulus (ratio between green MOE and basic density *BD*) and even maturation stress using only basic density for hardwood or softwood normal wood. The proportionality is true within a tree in all cases, hence *GSI* can be directly used for biomechanical studies at tree level.

Basic specific modulus (SM_b) and longitudinal shrinkage (*LS*) as well as maturation strain (α_m) are properties of cell wall material in the longitudinal direction depending only on the last fibre living phase (maturation phase, i.e. secondary wall deposition). Microfibril angle (*MFA*) in the secondary wall and chemical composition of cell wall polymers are the underlying parameters explaining the variations of these 3 properties. α_m provides a continuum of wood types from CW to TW through NW, but the analysis of SM_b and *LS* proves that RW cannot be considered as extreme case of NW but specific patterns as suggested by genomic studies. Predictive models should be built separately for the 3 types, but the pertinent combined data on α_m, *MFA* and chemistry of main polymers is lacking mainly for NW which has an important contribution to muscular function of the living wood, even in posture regulation. For CW (Yeh et al 2005) and for non G-layer TW (Baillères et al 1995) the relative composition in lignin monomers (H/G for softwoods, S/G for hardwoods) was a good predictor of RW. These parameters can be active also within NW without too much changes in lignin content.

By creating forces, the living wood generates tensile residual stresses within the internal skeleton, improving its resistance to flexure forces as wind action on the compressive side where the resistance to compression is lower. But high compression pre-stressing on one side or very high tension pre-stressing on the other side by RW will bring dangerous situations in case of strong wind in the axis of RW. There is a necessary trade-off between efficient posture control (by forces) and efficient pre-stressing (by stresses) and compression wood solution (the most dangerous under wind action) is managed by a complex simultaneous regulation of strain, modulus of elasticity (via the *MFA*), stress (via the density), force (via the ring width) and global geometry (via the anisotropy of second moment of area of the section).

References

Alméras T, Thibaut A, Gril J. 2005b. Effect of circumferential heterogeneity of wood maturation strain, modulus of elasticity and radial growth on the regulation of stem orientation in trees. Trees Structure and function 19 (4), 457–467. Trees Structure and function

Alméras T, Derycke M, Jaouen G, Beauchêne J, Fournier M. 2009. Functional diversity in gravitropic reaction among tropical seedlings in relation to ecological and developmental traits. Journal of Experimental Botany 60, 4397–4410.

Alméras T, Clair B. 2016*.* Critical review on the mechanisms of maturation stress generation in trees. Journal of The Royal Society Interface 13(122) , 20160550

Alméras T., Jullien D., Gril G. 2018. Modelling, Evaluation and Biomechanical Consequences of Growth Stress Profiles Inside Tree Stems. Anja Geitmann, Joseph Gril. Plant Biomechanics. From Structure to Function at Multiple Scales, Springer International Publishing, pp.21-48

Archer RR. 1984. Application of a new method for the growth stress measurement for Pinus Caribea. IUFRO P5-01, Properties and utilisation of tropical woods, Manaus, Brasil, 19 – 23/11/1984

Baillères H. 1994. Précontraintes de Croissance et Propriétés Mécanophysiques de Clones d'Eucalyptus (Pointe Noire–Congo): Hétérogénéités, Corrélations et Interprétations Histologiques. Thèse Université Bordeaux I, 162 p

Baillères H., Chanson B., Fournier M., Tollier MT., Monties B. 1995. Structure, composition chimique et retraits de maturation du bois chez les clones d'Eucalyptus. Annales des sciences forestières, 52 (2) 157-172.

Bordonné P.A. 1989. Module dynamique et frottement intérieur dans le bois: mesures sur poutres flottantes en vibrations naturelles. Thèse de Doctorat en Sciences du Bois, Institut National Polytechnique de Lorraine.

Brancheriau L., Baillères H. 2002. Natural vibration analysis of clear wooden beams: a theoretical review. Wood Science and Technology (36), 347-365

Brémaud I, Ruelle J, Thibaut A, Thibaut B. 2013. Changes in vibrational properties between compression and normal wood, roles of microfibril angle and of lignin. Holzforschung 67, 75–85

Brennan M, McLean JP, Altaner CM, Ralph J, Harris PJ. 2012. Cellulose microfibril angles and cell-wall polymers in different wood types of Pinus radiate. Cellulose 19, 1385–1404

Cave ID. 1972. A theory of the shrinkage of wood. Wood Science and Technology (6), 284-292

Cave ID., Hutt L. 1968. Anisotropic elasticity of plant cell wall. Wood Science & Technology 2:268–278

Clarke SH. 1937. The distribution, structure and properties of tension wood in beech (Fagus sylavatica L.). Forestry 11(2): 85-91

Clair B, Ruelle J, Beauchêne J, Prévost MF, Fournier M. 2006. Tension wood and opposite wood in 21 tropical rain forest species. 1. Occurrence and efficiency of the G-layer. IAWA Journal 27 (3), 329–338

Clair B, Alteyrac J, Gronvold A Espejo J, Chanson B, Alméras T. 2013. Patterns of longitudinal and tangential maturation stresses in Eucalyptus nitens plantation trees. Annals of forest science 70, 801–811

Clair B., Thibaut B. 2014. Chapter 6 Physical and Mechanical Properties of Reaction Wood. B. Gardiner et al. eds. The Biology of Reaction Wood, Springer Series in Wood Science, DOI 10.1007/978-3-642-10814-3_3

Cockrell RA., Knudson RM. 1973. A comparison of static bending, compression and tension parallel to grain and toughness properties of compression wood and normal wood of a Giant Sequoia. Wood Science and Technology 7, 241–250

Côté WA, Day AC, Timell TE. 1969. A contribution to the ultrastructure of tension wood fibres. Wood Science and Technology 3, 257–271

Coutand C, Fournier M, Moulia B. 2007. Gravitropic response of polar trunk: key roles of the regulation of wood restressing and of relative kinetics of cambial growth versus wood maturation. Plant Physiology 144, 1166–1180.

Cowdrey DR., Preston RD. 1966 Elasticity and microfibrillar angle in wood of Sitka spruce. Proc Roy Soc B 166:245–272

Cuny HE, Rathgeber CBK, Lebourgeois F, Fortin M, Fournier M, 2012. Life strategies in intra-annual dynamics of wood formation: example of three conifer species in a temperate forest in north-east France. *Tree Physiology* 32, 612–625.

Dadswell HE, Wardrop AB. 1955. The structure and properties of tension wood. Holzforschung 9, 97–103

Deleuze C., Houllier F. 1997. A transport model for tree ring width. Silva Fennica 31 (3): 239-250.

Fagerstedt KV, Mellerowicz E, Gorshkova T, Ruel K, Joseleau JP. 2014. Chapter 3 Cell Wall Polymers in Reaction Wood. B. Gardiner et al. eds. The Biology of Reaction Wood, Springer Series in Wood Science, DOI 10.1007/978-3-642-10814-3_3

Fang CH, Clair B, Gril J, Liu SQ. 2008. Growth stresses are highly controlled by the amount of G-layer in poplar tension wood. IAWA Journal 29 (3), 237–246

Fourcaud T., Zhang X., Stokes A., Lambers H., Körner C. 2008. Plant Growth Modelling and Applications: The Increasing Importance of Plant Architecture in Growth Models. Annals of Botany 101: 1053–1063, 2008

Fournier M, Chanson B, Thibaut B, Guitard D. 1994b. Measurements of residual growth strains at the stem surface observations on different species. Annals of forest science 51, 249–266

Fournier M, Bailleres H, Chanson B. 1994a. Tree biomechanics, growth, cumulative prestresses, and reorientations. Biomimetics 2, 229–251

Fournier M, Alméras T, Clair B, Gril J. 2014. Chapter 5 Biomechanical action and biological functions. The biology of reaction wood. eds B Gardiner, J Barnett, P Saranpää, J Gril , pp. 139–170. Berlin, Germany, Springer.

Funda T., Fundova I., Gorzsás A., Fries A., Wu HX. 2020. Predicting the chemical composition of juvenile and mature woods in Scots pine (*Pinus sylvestris* L.) using FTIR spectroscopy. Wood Science and Technology 54:289–311

Gardiner B, Barnett J, Saranpää P, Gril J. 2014. The biology of reaction wood. Springer, Berlin, Heidelberg

Gibson L.J., Ashby M.F. 1999. Cellular Solids: Structure and Properties, Cambridge University Press, 2nd edition.

Ghislain B., Engel J., Clair B. 2019. Diversity of anatomical structure of tension wood among 242 tropical tree species. IAWA journal. 40(4) 765-784

Gindl W. (2001) The effect of lignin on the moisture-dependent behaviour of spruce wood in axial compression. JOURNAL OF MATERIALS SCIENCE LETTERS 20, 2161 – 2162

Gindl W., Teischinger A. (2002) Axial compression strength of Norway spruce related to structural variability and lignin content. Composites: Part A 33, 1623–1628

Glass SV, Zelinka SL. 2010. Chapter 4, Moisture relations and physical properties of wood in Wood handbook—Wood as an engineering material. General Technical Report FPL-GTR-190. USDA, Forest Service, Forest Products Laboratory.

Gordon JE. 1978. Structures, or why things don't fall down. Penguin Books, Harmondsworth

Gorshkova T, Brutch N, Chabbert B, Deyholos M, Hayashi T, Lev-Yadun S, Mellerowicz EJ , Morvan C, Neutelings G, Pilate G. 2012. Plant fibre formation, state of the art, recent and expected progress, and open questions. Critical Review in Plant Sciences 31, 201–228

Gorshkova T, Chernova T, Mokshina N, Ageeva M, Mikshina P. 2018. Plant "muscles", fibers with a tertiary cell wall. New Phytologist 218 (1), 66–72

Gril J., Jullien D., Bardet S., Yamamoto H. 2017. Tree growth stress and related problems. Journal of Wood Science, 63 (5), pp. 411-432.

Guitard D., El Amri F., Modèles prévisionnels du comportement élastique tridimensionnel des bois feuillus ou résineux, Annales des Sciences Forestières 44 (1987) 335–358.

Huang YS., Chen SS., Lin TP., Chen YS. 2001. Growth stress distribution in leaning trunks of *Cryptomeria japonica.* Tree Physiology 21, 261–266

Jourez B., Riboux A., Leclercq A. 2001a. Comparison of basic density and longitudinal shrinkage in tension wood and opposite wood in young stems of Populus euramericana cv. Ghoy when subjected to a gravitational stimulus. Canadian journal of forest research 31(10):1676-1683

Jourez B., Riboux A., Leclercq A. 2001b. Anatomical characteristics of tension wood and opposite wood in young inclined stems of poplar (*Populus euramericana* CV 'Ghoy'). IAWA J. 22: 133–157.

Jullien D, Widmann R, Loup C, Thibaut B. 2013. Relationship between tree morphology and growth stress in mature European beech stands. Annals of forest science 70 (2), 133–142

Kretschmann DE. 2010. Chapter 5, Mechanical properties of wood. Wood handbook—Wood as an engineering material. General Technical Report FPL-GTR-190. USDA, Forest Service, Forest Products Laboratory.

Leonardon M, Altaner CM, Vihermaa L, Jarvis MC. 2010. Wood shrinkage, influence of anatomy, cell wall architecture, chemical composition and cambial age. European journal of wood and wood products 68, 87-94

Mellerowicz EJ, Baucher M, Sundberg B, Boerjan W. 2001. Unravelling cell wall formation in the woody dicot stem. Plant Molecular Biology 47 1-2, 239-274.

Moulia B, Coutand C, Lenne C. 2006. Posture control and skeletal mechanical acclimation in terrestrial plants: implications for mechanical modeling of plant architecture. Am. J.

Nanayakkara B., Manley-Harris M., Suckling I.D., Donaldson LA. 2009. Quantitative chemical indicators to assess the gradation of compression wood. Holzforschung 63:431 – 439.

Okuyama T., Yamamoto H., Yoshida M., Hattori Y., Archer RR. 1994. Growth stresses in tension wood, role of microfibrils and lignification. Annals of forest science 51, 291–300.

Pillow MY., Luxford RF. (1937) Structure, occurrence and properties of compression wood. Technical bulletin N° 546, USDA, Washington, 32p.

Plomion C, Leprovost G, Stokes A. 2001. Wood formation in trees. Plant Physiology 127 (4), 1513-1523.

Ruelle J. 2014. Chapter 2 Morphology, Anatomy and Ultrastructure of Reaction Wood. B. Gardiner et al. eds. The Biology of Reaction Wood, Springer Series in Wood Science, DOI 10.1007/978-3-642-10814-3_3

Ruelle J, Yamamoto H, Thibaut B. 2007. Growth stresses and cellulose structural parameters intension and normal wood from three tropical rainforest angiosperm species. Bioresources, 235–251

Thibaut B., Gril J., Fournier M. 2001. Mechanics of wood and trees, some new highlights for an old story. Comptes Rendus de l'Académie des Sciences Paris, série II B 329 (9), 701–716

Thibaut B., Gril J. 2003. Growth stresses. In: Barnett JR, Jeronimidis G (eds) Wood quality and its biological basis. Blackwell, Oxford, pp 137–156

Thibaut B. 2019. Three-dimensional printing, muscles and skeleton: mechanical functions of living wood, Journal of Experimental Botany, Volume 70, Issue 14, 1 July 2019, Pages 3453–3466

Timell TE. 1986. Compression wood in gymnosperms, 3 vol. Springer, Berlin, 2210 pp

Trouvé R., Bontemps JD., Seynave I., Collet C., Lebourgeois F. 2015. Stand density, tree social status and water stress influence allocation in height and diameter growth of Quercus petraea. Tree Physiology 35, 1035–1046

Vieilledent G, Fischer FJ, Chave J, Guibal D, Langbour P, Gérard J (2018). New formula and conversion factor to compute basic wood density of tree species using a global wood technology database. American Journal of Botany 105(10): 1–9.

Watanabe U., Norimoto M. 1996. Shrinkage and elasticity of normal and compression wood in conifers. Mokuzai Gakkaishi 42 (7), 651-658

Yamamoto H., Okuyama T. 1988. Analysis of the generation process of growth stresses in cell walls. Mokuzai Gakkaishi 34 (10), 788-793

Yamamoto H., Okuyama T., Sugiyama K., Yoshida M. 1991. Generation process of growth stresses in cell walls III. Growth stress in compression wood. Mokuzai Gakkaishi 37 (2), 94-100

Yamamoto H., Okuyama T., Yoshida M. 1998. Growth stress generation and microfibril angle in reaction wood. In: Butterfield BG (ed) Microfibril angle in wood. International Association of Wood Anatomist, Christchurch, pp 225–239

Yamamoto H., Sassus F., Ninomiya M, Gril J. 2001. A model of anisotropic swelling and shrinking process of wood. Part 2. A simulation of shrinking wood. Wood Science and Technology 35: 167-181

Yamashita S., Yoshida M., Takayama S. , T. Okuyama T. 2007. Stem-righting mechanisms in gymnosperm trees deduced from limitations in compression wood development. Annals of Botany. 99 487–493.

Yang JL, Baillères H, Okuyama T, Muneri A, Downes G. 2005. Measurement methods for longitudinal surface strain in trees, a review. Australian Forestry 68, 34–43

Yeh TF, Goldfarb B, Chang HM, Peszlen I, Braun JL, Kadla JF. 2005. Comparison of morphological and chemical properties between juvenile wood and compression wood of loblolly pine. Holzforschung 59, 669–674

Yeh TF, Braun jL, Goldfarb B, Chang HM, Kadla, J.F. 2006. Morphological and chemical variations between juvenile wood, mature wood, and compression wood of loblolly pine (*Pinus taeda* L.). Holzforschung. 60, 1-8

Yoshida M, Okuda T, Okuyama T. 2000. Tension wood and growth stress induced by artificial inclination in *Liriodendron tulipifera* Linn. and *Prunus spachiana Kitamura* f. ascendens Kitamura. Annals of forest science 57 (8), 739–746

Yoshida M, Okuyama T. 2002. Techniques for measuring growth stress on the xylem surface using strain and dial gauges. Holzforschung 56 (5), 461–467